Biochimica et Biophysica Acta 1817 (2012) 336–352

Contents lists available at SciVerse ScienceDirect

Biochimica et Biophysica Acta

journal homepage: www.elsevier.com/locate/bbabio

Cross-species investigation of the functions of the *Rhodobacter* PufX polypeptide and the composition of the RC–LH1 core complex

Lucy I. Crouch, Michael R. Jones *

School of Biochemistry, Medical Sciences Building, University of Bristol, University Walk, Bristol, BS8 1TD, UK

ARTICLE INFO

Article history:
Received 9 August 2011
Received in revised form 24 October 2011
Accepted 27 October 2011
Available online 3 November 2011

Keywords:
Photosynthesis
Rhodobacter sphaeroides
Reaction centre
Light harvesting
PufX
LH1 antenna

ABSTRACT

In well-characterised species of the *Rhodobacter* (*Rba.*) genus of purple photosynthetic bacteria it is known that the photochemical reaction centre (RC) is intimately-associated with an encircling LH1 antenna pigment protein, and this LH1 antenna is prevented from completely surrounding the RC by a single copy of the PufX protein. In *Rba. veldkampii* only monomeric RC–LH1 complexes are assembled in the photosynthetic membrane, whereas in *Rba. sphaeroides* and *Rba. blasticus* a dimeric form is also assembled in which two RCs are surrounded by an S-shaped LH1 antenna. The present work established that dimeric RC–LH1 complexes can also be isolated from *Rba. azotoformans* and *Rba. changlensis*, but not from *Rba. capsulatus* or *Rba. vinaykumarii*. The compositions of the monomers and dimers isolated from these four species of *Rhodobacter* were similar to those of the well-characterised RC–LH1 complexes present in *Rba. sphaeroides*. Pigment proteins were also isolated from strains of *Rba. sphaeroides* expressing chimeric RC–LH1 complexes. Replacement of either the *Rba. sphaeroides* LH1 antenna or PufX with its counterpart from *Rba. capsulatus* led to a loss of the dimeric form of the RC–LH1 complex, but the monomeric form had a largely unaltered composition, even in strains in which the expression level of LH1 relative to the RC was reduced. The chimeric RC–LH1 complexes were also functional, supporting bacterial growth under photosynthetic conditions. The findings help to tease apart the different functions of PufX in different species of *Rhodobacter*, and a specific protein structural arrangement that allows PufX to fulfil these three functions is proposed.

1. Introduction

The purple photosynthetic bacterium *Rhodobacter (Rba.) sphaeroides* has provided many insights into the molecular mechanisms underlying photosynthetic energy transduction. Light-driven charge separation is catalysed in a reaction centre (RC) that is surrounded by a light-harvesting 1 (LH1) pigment protein. This LH1 antenna is made up from multiple copies of single membrane-spanning α- and β-polypeptides that encase bacteriochlorophyll (BChl) and carotenoid pigments [1–10]. These so-called RC–LH1 core complexes are associated with a peripheral antenna formed from light-harvesting 2 (LH2) pigment proteins [11,12]. The RC–LH1 complex assembles in the photosynthetic membrane in two forms, a monomeric version in which the RC is surrounded by a C-shaped LH1 aggregate (when viewed perpendicular to the membrane) and a dimeric version displaying two-fold symmetry where two RCs are surrounded by an S-shaped LH1 aggregate [13]. To date, dimeric complexes have been documented in *Rba. sphaeroides* by electron microscopy (EM) of isolated proteins [13–15] and atomic force microscopy (AFM) of membranes [16,17] and in a second species, *Rba. blasticus*, by AFM of membranes [18]. In contrast, the RC–LH1 complex has been reported to be exclusively monomeric in *Rba. veldkampii*, as judged by AFM of intact membranes and cryo-EM of isolated complexes [19,20].

An additional component of the *Rba. sphaeroides* RC–LH1 complex is a polypeptide termed PufX which is present at a stoichiometry of one per RC–LH1 monomer (see [21] for a review). This protein has a single membrane-spanning α-helix and appears to prevent the LH1 antenna from completely encircling the RC [14,22], which is the case in some other species of purple bacteria where there is no evidence of a PufX or equivalent polypeptide [23–27]. Removal of the gene encoding PufX from the *Rba. sphaeroides* genome results in the assembly of exclusively monomeric RC–LH1 complexes in which the RC is completely surrounded by a closed ring of LH1 pigment protein [14,22], and loss of the ability of the organism to grow under standard photosynthetic conditions [28–30]. In experiments with *Rba. sphaeroides* it has been found that the truncation of the N-terminus of PufX leads to a loss of the dimeric form of the RC–LH1 complex [31,32] and there is a general consensus that PufX is a major factor dictating whether dimeric RC–LH1 complexes are assembled in this species. However the RC–LH1 complex of *Rba. veldkampii* is exclusively monomeric despite the fact that this

Abbreviations: AFM, atomic force microscopy; A_{LH1}/A_{RC}, ratio of LH1 absorbance to RC absorbance; BChl, bacteriochlorophyll; DM, decyl β-D-maltoside; DDM, n-dodecyl-β-D-maltoside; DHPC, 1,2-diheptanoyl-*sn*-glycero-3-phosphocholine; EM, electron microscopy; LDAO, N,N-dimethyldodecylamine N-oxide; LH1, light-harvesting 1 pigment protein; LH2, light-harvesting 2 pigment protein; NMR, nuclear magnetic resonance; OG, octyl β-D-glucoside; PDB, Protein Data Bank; PMS, phenazine methosulphate; RC, reaction centre; *Rba*, *Rhodobacter*; *Rps*, *Rhodopseudomonas*

* Corresponding author. Tel.: +44 117 3312135; fax: +44 117 3312168.
E-mail address: m.r.jones@bristol.ac.uk (M.R. Jones).

0005-2728/$ – see front matter © 2011 Elsevier B.V. All rights reserved.
doi:10.1016/j.bbabio.2011.10.009

species also possesses a PufX [19,20], and it would therefore appear that the assembly of dimeric RC–LH1 complexes is not simply dictated by the presence of PufX *per se*, but is dependent on other factors.

It is not yet clear why some *Rhodobacter* species assemble dimeric RC–LH1 core complexes while others do not, and what advantage (s) the dimeric architecture confers. Monomeric RC–LH1 complexes are visible in AFM images of membranes of *Rba. sphaeroides*, forming a minor population alongside the major population of dimeric RC–LH1 complexes [16,33]. A systematic, quantitative analysis of the relative amounts of monomer and dimer in AFM images of *Rba. sphaeroides* membranes has not been carried out to date. In large membrane patches from *Rba. blasticus* formed by fusion of smaller fragments in two freeze–thaw cycles, 75% of the observed RC–LH1 complexes were dimeric and the remainder monomeric [18], but it was not possible to determine whether the monomers were produced from the dimers during sample preparation, or whether the two forms existed in equilibrium in intact bacterial cells. It is clear that PufX determines the open architecture of the *Rba. sphaeroides* RC–LH1 complex, enlarged and closed rings of LH1 being seen for PufX-deficient RC–LH1 complexes in AFM topographs and in EM data [14,22]. Such PufX-deficient complexes are exclusively monomeric, the open architecture seen in PufX-containing RC–LH1 complexes being required for dimerisation. Studies of the impact of these different architectures for the RC–LH1 complex on cyclic electron transfer in the photosynthetic membrane have focussed on the effects of removal of PufX and the resulting closed structure for the LH1 antenna [34–36], and to date there has been no attempt to determine whether the monomeric and dimeric forms of the RC–LH1 complex result in differences in the characteristics of cyclic electron transfer. A complication is uncertainty over the relative populations of RC–LH1 monomers and dimers in a particular type of strain grown under particular conditions, available data being limited to a handful of studies employing either sucrose gradient fractionation of detergent-isolated complexes [17,32,37] or analysis of patches of intact membrane by AFM or EM [14–16,31].

The finding that the RC–LH1 complex from *Rba. sphaeroides* assembles in a dimeric form whereas that from *Rba. veldkampii* is exclusively monomeric has raised the question of which component(s) of the complex are responsible for this difference. Particular attention has been focussed on PufX, as a feature of this polypeptide is the relatively low degree of sequence identity displayed across the *Rhodobacter* genus [38]. Alignment of the five available PufX sequences shows only eight absolutely conserved residues in a protein of between 75 and 83 amino acids (see [21] for a discussion). The PufX from *Rba. sphaeroides* shows a high degree of identity with that from *Rba. azotoformans* (89% — see Table 1), but much lower identity with the PufX proteins from *Rba. blasticus* (26%), *Rba. veldkampii* (23%) and *Rba. capsulatus* (23%). The latter three percentage identities are much lower than those for the RC and LH1 polypeptides that make up the remainder of the corresponding RC–LH1 complex (Table 1).

Table 1
Identity between the sequences of the component polypeptides of the RC–LH1 core complex from *Rba. sphaeroides* and other *Rhodobacter* species where the sequence of PufX is known.[a].

Rba. sphaeroides protein	Encoding gene	Percentage identity			
		Rba. azotoformans	*Rba. blasticus*	*Rba. veldkampii*	*Rba. capsulatus*
LH1 β (PufB)	*pufB*	–	–	–	79
LH1 α (PufA)	*pufA*	–	–	–	77
RC L (PufL)	*pufL*	95	80	70	78
RC M (PufM)	*pufM*	96	77	74	76
RC H (PuhA)	*puhA*	–	–	–	61
PufX	*pufX*	89	26	23	23

[a] Determined using Swiss-Prot [74] to search for relevant sequences and ClustalW [75] to align and calculate percentage identity. No entry indicates relevant gene sequence was not available.

Taken together with the loss of dimeric RC–LH1 complexes that accompanies the deletion of PufX in *Rba. sphaeroides*, the finding that some species of *Rhodobacter* assemble dimers but others do not has led to attempts to use PufX sequence alignments to identify a "dimerisation motif". The low identity between the five available PufX sequences makes it challenging to identify specific residues that could dictate whether the RC–LH1 complex will be dimeric or monomeric, but specific proposals have been made and these are detailed in the Discussion. Some of the logic underlying these proposals is based on the premise that the RC–LH1 complex from both *Rba. capsulatus* and *Rba. azotoformans* assembles in the dimeric form, an assumption that has not been tested experimentally. One aim of the present study was therefore to look for evidence of dimeric RC–LH1 complexes in these two species, and also address the wider question of how common the dimeric variant of the RC–LH1 complex is within the *Rhodobacter* genus by examining the pigment-protein content of two newly characterised species, *Rba. changlenesis* [39] and *Rba. vinaykumarii* [40].

The second aim of the present study was to further investigate the factors that dictate whether the RC–LH1 complex assembles in a dimeric form by utilising strains of *Rba. sphaeroides* that contain chimeric pigment-protein complexes. In previous work [41] it was reported that photosynthetic growth was retained in a *Rba. sphaeroides* strain where the native PufX had been replaced with the PufX from *Rba. capsulatus* (a strain termed RCLH1sXc), despite the limited sequence identity between the two (Table 1). The spectral characteristics of the membrane-embedded RC–LH1 complex from the RCLH1sXc strain were similar to those of the native complex and the strain was also able to grow photosynthetically, which implied that some of the roles of the native PufX could be fulfilled by the *Rba. capsulatus* variant [41]. Also produced in this work were strains heterologously expressing the *Rba. capsulatus* LH1 antenna alongside either the *Rba. sphaeroides* PufX, the *Rba. capsulatus* PufX or no PufX [41]. The present work examines whether dimeric RC–LH1 core complexes are assembled in these strains of *Rba. sphaeroides* expressing non-native LH1 and/or PufX proteins, and studies in more detail the composition and functionality of their chimeric RC–LH1 complexes.

2. Materials and methods

2.1. Sources and growth of native bacterial strains

Wild-type strains *Rba. sphaeroides* NCIB8253 and *Rba. capsulatus* Kb-1 were revived from laboratory stocks. *Rba. azotoformans* (JCM number 9340) was obtained from the Japan Collection of Microorganisms (RIKEN Bioresource Centre). Native strains of *Rba. changlensis* and *Rba. vinaykumarii* were kindly donated by Dr. Sasikala from the Jawaharlal Nehru Technological University in Hyderabad, India. The LH2-deficient *Rba. sphaeroides* strain DBCΩ was also used [42], which is strain NCIB8253 with the LH2-encoding *puc* operon replaced by a cassette conferring resistance to streptomycin.

Rba. sphaeroides NCIB8253 and *Rba. changlensis* were grown in M22 + medium [43] and *Rba. capsulatus* Kb-1 was grown in RCV-PY medium [44]. *Rba. azotoformans* was grown in MMYS medium (Japanese Collection of Microorganisms website (http://www.jcm.riken.jp/)) and *Rba. vinaykumarii* was also grown in this medium supplemented with 68 mM sodium glutamate and 137 mM glycerol. *Rba. sphaeroides* was grown at 34 °C and the remaining species were grown at 30 °C.

For growth under dark/semi-aerobic conditions a 10 ml aliquot of the relevant medium in a 30 ml universal bottle was inoculated with cells from a freeze-dried stock, glycerol stock or agar plate and placed in an orbital incubator at 180 rpm for 24 h. These 10 ml starter cultures were then used to inoculate 70 ml of medium in a 100 ml Erlenmeyer

flask, and these intermediate cultures were grown for 24 h at 180 rpm and used to inoculate 1.5 L of medium in a 2 L Erlenmeyer flask. These final large cultures were grown for ~36 h at 180 rpm before harvesting cells by centrifugation.

Growth under anaerobic/illuminated conditions was carried out initially in completely-filled 18 ml screw-top culture tubes that were inoculated directly from stocks as above or from a 70 ml intermediate culture grown under dark/semi-aerobic conditions. The culture tubes were incubated for 24 h in a glass circulating water bath that was illuminated by four 100 W incandescent light bulbs and then used to inoculate completely-filled 1 l Roux bottles that were incubated under the same conditions for 2–3 days. For growth under high illumination conditions the light bulbs were replaced by three 500 W tungsten halogen floodlamps.

2.2. Construction and growth of modified strains of Rba. sphaeroides

The plasmids used to express chimeric RC–LH1 complexes were identical to those described in previous work [41], comprising different combinations of the LH1 *pufBA*, RC *pufLM* and *pufX* genes from *Rba. sphaeroides* and *Rba. capsulatus* cloned as an intact *pufBALMX* operon into the broad-host range vector pRK415 that confers resistance to tetracycline. Four different plasmids were used, all containing the *Rba. sphaeroides pufLM* genes. Plasmid pRKEHLH1cXs contained *pufBA from Rba. capsulatus* and *pufX* from *Rba. sphaeroides*, plasmid pRKEHLH1cXc contained *pufBA* and *pufX* from *Rba. capsulatus*, plasmid pRKEHLH1sXc contained *pufBA genes from Rba. sphaeroides* and *pufX* from *Rba. capsulatus*, and plasmid pRKEHLH1cX$^-$ contained *pufBA genes from Rba. capsulatus and lacked a pufX* gene.

The plasmids were inserted into the *Rba. sphaeroides* deletion strains DPF2/G and DD13/G [42] through conjugative crossing [43]. Strain DPF2 is native strain NCIB8253 with the *pufBALMX* operon replaced by a cassette conferring resistance to neomycin [45], and DPF2/G is a spontaneously-occurring variant of DPF2 with an undefined mutation that causes expression of green carotenoids. Strain DD13 is DPF2 with additional replacement of the LH2-encoding *puc* operon replaced by a cassette conferring resistance to streptomycin [42], and DD13/G is a spontaneously-occurring variant of DD13 with an undefined mutation that causes expression of green carotenoids [42]. The control strains used were DPF2/G and DD13/G complemented with plasmid pRKEH10 containing the *Rba. sphaeroides pufBALMX* operon or plasmid pRKEH10X$^-$ which is a derivative of pRKEH10 lacking *pufX*.

Growth of the engineered strains of *Rba. sphaeroides* was carried out as described above for wild-type NCIB8253 except the medium was supplemented with neomycin, streptomycin and tetracycline where appropriate, as described previously [46]. Tetracycline was not used for growth under photosynthetic conditions to avoid the production of reactive oxygen species that results from its photodegradation.

2.3. Preparation of membranes, pigment-protein solubilisation and fractionation

Photosynthetic membranes were extracted from cells using a French pressure cell, as described in [47]. Pigment proteins were solubilised from these membranes by a protocol using 4% n-dodecyl-β-D-maltoside (DDM) [15], as described in detail recently [46]. Solubilised pigment proteins were fractionated by ultracentrifugation on 20–25% (w/v) five-step sucrose density gradients, as also described in detail recently. After photography, sucrose gradients were either fractionated for analysis by absorbance spectroscopy or intact gradients were scanned at 1 mm intervals along their length using a PerkinElmer Lambda35 spectrophotometer fitted with a fibre optic attachment [46].

3. Results

3.1. Do Rba. capsulatus and Rba. azotoformans assemble dimeric RC–LH1 core complexes?

The use of protein sequence alignments to identify residues of PufX that are key to the formation of RC–LH1 dimers requires knowledge of whether dimers are assembled in each of the five species where the sequence of PufX has been determined, knowledge which is not available for *Rba. capsulatus or Rba. azotoformans*. Accordingly, the profile of pigment-protein complexes in *Rba. capsulatus* and *Rba. azotoformans* were compared with that from *Rba. sphaeroides*. This was achieved by extraction of the RC–LH1 and LH2 complexes from intracytoplasmic membranes using the mild detergent DDM, and fractionation by sucrose density gradient ultracentrifugation. The result of fractionating solubilised pigment proteins from *Rba. sphaeroides* NCIB8253, *Rba. capsulatus* Kb-1 and *Rba. azotoformans* 9340 grown under photosynthetic conditions is shown in Fig. 1A.

Either three or four pigmented bands were obtained in each sucrose gradient, and the content of each band was identified by absorbance spectroscopy. The faint orange band at the top of each gradient in Fig. 1A was attributable to free carotenoid (spectra not shown); under this growth condition the principal carotenoid in *Rba. sphaeroides* is spheroidene, and the spectra from all three gradients were consistent with this. The intense green–brown band below this was attributable to the peripheral LH2 antenna (spectra not

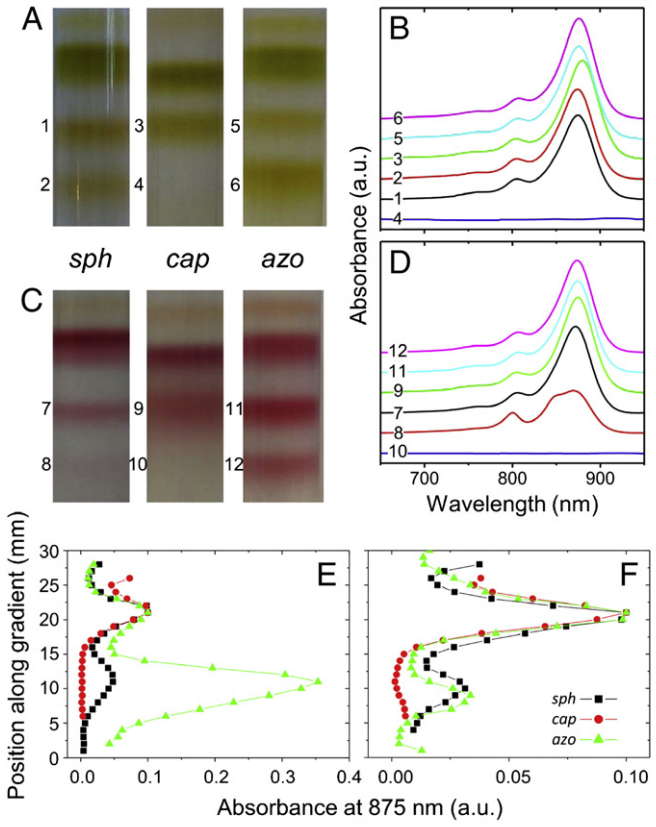

Fig. 1. Sucrose gradient fractionation and absorbance spectra of solubilised pigment proteins from wild-type *Rba. sphaeroides, Rba. capsulatus and Rba. azotoformans*. (A) Fractionated pigment proteins and (B) corresponding absorbance spectra for material from cells grown under light conditions. (C) Fractionated pigment proteins and (D) corresponding absorbance spectra for material from cells grown under dark conditions. Numbers indicate the approximate position of fractions removed for spectroscopy, and resulting spectra. (E,F) Absorbance at 875 nm from spectra recorded at 1 mm intervals along gradients of the type shown in A and B, respectively. For comparison, profiles have been normalised at the maximum of the upper band corresponding to monomeric RC–LH1 complexes. Key: *sph*— *Rba. sphaeroides*, *cap*— *Rba. capsulatus*, *azo*— *Rba. azotoformans*.

shown). The LH2 fraction consistently ran as two closely-spaced bands for *Rba. sphaeroides* (Fig. 1A, left) and *Rba. azotoformans* (Fig. 1A, right), whereas for *Rba. capsulatus* (Fig. 1A, centre) the LH2 fraction ran as a single band corresponding to the lower of the two bands in the other two species. The two LH2 bands obtained for *Rba. sphaeroides* have been previously attributed to two differently sized LH2 pigment proteins of 7 and 12 nm diameter [48]. The remaining two khaki-coloured bands in the gradients loaded with *Rba. sphaeroides* pigment protein (Fig. 1A) are attributable to monomeric (upper-numbered 1) and dimeric (lower-numbered 2) RC–LH1 complexes [17,32,37], and an equivalent profile was obtained with *Rba. azotoformans* (Fig. 1A, right). In contrast the gradient loaded with complexes from *Rba. capsulatus* had only the band corresponding to monomeric RC–LH1 core complexes, with no obvious indication of the presence of dimers (Fig. 1A, centre).

Gradients of the type shown in Fig. 1A were analysed either by carefully removing an aliquot from the centre of each band (at the positions indicated by the numbers) and recording an absorbance spectrum, or by recording absorbance spectra at 1 mm intervals along the length of an intact gradient using a spectrophotometer fitted with a pair of optical fibres (see Materials and methods). The latter method was used to quantify the relative amounts of monomeric and dimeric RC–LH1 complex (see below). The absorbance spectrum of the *Rba. sphaeroides* RC–LH1 complex is a composite of RC bands at 760, 805 and 867 nm (an example of an RC spectrum is given in Fig. 3B), and a dominant LH1 band at approximately 870 nm which masks the RC 867 nm band. The LH2 antenna exhibits an absorbance band at around 800 nm and a somewhat more intense band at 850 nm.

Fig. 1B shows absorbance spectra of aliquots removed from the gradients in Fig. 1A at the positions indicated by the numbers. For the purposes of comparison the spectra in Fig. 1B were corrected for a small amount of baseline scatter between 650 and 950 nm, normalized to an absorbance of 0.1 at the maximum of the 805 nm absorbance band, and then stacked. As reported previously, the spectra of monomeric and dimeric *Rba. sphaeroides* RC–LH1 complexes were similar to one another (Fig. 1B, spectra 1 and 2), and spectra of both forms of the *Rba. azotoformans* RC–LH1 were also similar (Fig. 1B, spectra 5 and 6). The spectrum of the monomeric *Rba. capsulatus* complex (Fig. 1B, spectrum 3) showed a small increase in relative intensity of the LH1 band associated with a ~5 nm shift of its maximum to longer wavelengths relative to the spectrum of the *Rba. sphaeroides* monomer (Fig. 1B, spectrum 1). The average absorbance maxima of the LH1 component in these monomeric and dimeric complexes are listed in Table 2. The spectrum of aliquot 4 was essentially featureless (Fig. 1B, spectrum 4 — not normalized) indicating a lack of dimeric RC–LH1 complexes in the DDM extract from *Rba. capsulatus*.

A convenient and simple way to assess the composition of a RC–LH1 complex from its absorbance spectrum is to calculate the ratio between the maxima at ~875 nm and ~805 nm, which provides a number representative of the amount of LH1 BChl per RC (termed the A_{LH1}/A_{RC} ratio). Ratios from spectra recorded for multiple gradients of the type in Fig. 1A are reported in Table 2. In general the line-shape of the spectra recorded was highly reproducible, resulting in low standard deviations for the resulting A_{LH1}/A_{RC} ratios of around ± 0.2. For *Rba. sphaeroides* the A_{LH1}/A_{RC} ratios for monomeric RC–LH1 complexes from dark- and light-grown cells were similar at 4.23 and 4.36, respectively, and the equivalent values for *Rba. azotoformans* were 4.54 and 4.60. None of these values could be regarded as being significantly different from one another, given the associated standard deviations. For *Rba. capsulatus* these A_{LH1}/A_{RC} ratios were a little higher, at 4.77 and 4.91, respectively. Although this could be taken as an indication that the amount of LH1 per RC in *Rba. capsulatus* is greater than in *Rba. sphaeroides*, this ratio does not take into account species variations in the width of the LH1 band or its overlap with the underlying RC absorbance band at ~867 nm. As a result a cautious interpretation would be that the composition of the monomeric RC–LH1 complexes was similar in the three species, with no clear evidence of a significant difference. In general, the A_{LH1}/A_{RC} ratios obtained for RC–LH1 dimers were somewhat higher than the corresponding monomer for all three species (Table 2), but again the differences were not so great that one could conclude that there was a systematic difference in the amount of LH1 BChls per RC between monomers and dimers from these species.

Table 2 also summarises results from an analysis of multiple repeats of equivalent intact gradients to determine the percentage of the total population of RC–LH1 complex in the monomeric and dimeric form. As described previously (see Fig. 4 in [46]), absorbance spectra were recorded at 1 mm intervals along the length of each gradient, divided into monomer and dimer bins, and the total amount of monomer and dimer calculated from the sum of the 875 nm absorbance in the component spectra. Sample profiles are shown in Fig. 1E and F. The data showed that RC–LH1 complexes extracted from photosynthetically-grown *Rba. sphaeroides* cells comprised ~63% monomer and ~37% dimer, whereas those from photosynthetically-grown *Rba. azotoformans* cells comprised ~17% monomer and ~83% dimer (Table 2). RC–LH1 complexes from *Rba. capsulatus* cells were again exclusively monomeric with no hint of a dimeric form. It should be noted that this pattern of results was highly reproducible, being observed with several sets of gradients loaded with material originating from at least three separate cell cultures. Data shown in Table 2 are for at least four replicate gradients (actual numbers shown in brackets), and standard deviations were typically of the order of ± 6%.

3.2. Complexes in cells grown under dark/semi-aerobic conditions.

A useful feature of many purple bacteria is that the photosynthetic apparatus is assembled when cells are grown by aerobic respiration in the dark, provided that the oxygen level in the culture is not too

Table 2
Quantification of photosystem components resolved through sucrose density gradient fractionation of solubilised membranes from species of *Rhodobacter*.

Species	Growth	Percentage total population ± SD (n)[a]		Monomer		Dimer	
		% Monomer	% Dimer	A_{LH1}/A_{RC} ± SD (n)[a]	LH1 max[b] (nm)	A_{LH1}/A_{RC} ± SD (n)[a]	LH1 max[b] (nm)
Rba. sphaeroides	Dark	100 ± 0.0 (4)	0.0 ± 0.0 (4)	4.23 ± 0.11 (16)	872	–	–
	Light	62.9 ± 5.3 (5)	37.1 ± 5.3 (5)	4.36 ± 0.18 (10)	875	4.58 ± 0.53 (5)	873–874
Rba. capsulatus	Dark	100	0.0	4.77 ± 0.20 (5)	875	–	–
	Light	100	0.0	4.91 ± 0.18 (11)	880	–	–
Rba. azotoformans	Dark	63.0 ± 5.9 (5)	37.0 ± 5.9 (5)	4.54 ± 0.12 (10)	874	4.67 ± 0.17 (9)	874
	Light	16.6 ± 3.7 (9)	83.4 ± 3.7 (9)	4.60 ± 0.22 (13)	876	4.93 ± 0.21 (15)	876–877
Rba. changlensis	Dark	71.5 ± 7.1 (7)	28.5 ± 7.1 (7)	4.22 ± 0.15 (7)	873	4.30 ± 0.06 (2)	872
	Light	59.0 ± 6.1 (5)	41.0 ± 6.1 (5)	4.22 ± 0.14 (5)	874	LH2[c]	–
Rba. vinaykumarii	Dark	100	0.0	4.04 ± 0.48 (15)	870	–	–
	Light	100	0.0	3.72 ± 0.31 (10)	873–874	–	–

[a] n — number of gradients.
[b] Maximum of LH1 Q_y absorbance band.
[c] Pigmented band contaminated with LH2.

high. This enables extensive genetic manipulation of RCs and LH complexes, including the introduction of changes that would be lethal to cells growing under photosynthetic conditions. Fig. 1C shows sucrose density gradient fractionation of pigment proteins from cells of *Rba. sphaeroides*, *Rba. capsulatus* and *Rba. azotoformans* grown under dark/semi-aerobic conditions. The principal carotenoid accumulated in *Rba. sphaeroides* under these conditions is spheroidenone, producing a bright red colouration. For convenience, from this point on the two sets of growth conditions are simply referred to as "light" and "dark".

In general the pattern of results obtained with dark-grown cells was similar to that seen with light-grown cells, with *Rba. capsulatus* completely lacking dimeric RC–LH1 complexes (Fig. 1C, middle) and *Rba. azotoformans* having a pronounced pigmented band corresponding to dimers (Fig. 1C, right). Numbered spectra corresponding to particular positions on these gradients are shown in Fig. 1D, and absorbance maxima and A_{LH1}/A_{RC} ratios from these spectra are listed in Table 2. The most striking feature on comparing the data in Fig. 1A and C was that for both *Rba. sphaeroides* and *Rba. azotoformans* the prominence of the dimer band was reduced in the material extracted from dark-grown cells. In the case of *Rba. azotoformans* the relative amount of dimer was reduced from ~83% in light-grown cells to ~37% in dark-grown cells (Table 2), and this reduction was observed reproducibly across several bacterial cultures.

In addition to this, the absorbance spectrum of the band labelled 8 in Fig. 1C, corresponding to the expected position for RC–LH1 dimers, showed the presence of significant amounts of the *Rba. sphaeroides* LH2 antenna protein, with peaks at 800 nm (distinctly to the blue of the expected position for a RC band at ~805 nm) and 850 nm, as well as a shoulder at 875 nm attributable to LH1 (Fig. 1D, spectrum 8). This showed that this faint band was not attributable to just RC–LH1 dimers assembled in dark-grown *Rba. sphaeroides* cells, but rather to some more complex mixture of aggregated LH2 and RC–LH1 complexes. Similar spectra showing the presence of LH2 were also obtained on analysis of intact gradients, confirming that it was not an artefact of fractionation of the gradient. This LH2 contamination could not be removed by increasing the detergent concentration during solubilisation of the pigment proteins, changing the time or temperature for solubilisation or adding salt (data not shown). Given this the relative population of dimeric RC–LH1 complexes in dark-grown *Rba. sphaeroides* is assigned a value of zero in Table 2, although it is possible that some or all of the small amount of RC–LH1 complex seen co-migrating with aggregated LH2 could be the dimeric form.

3.3. Origin of monomeric RC–LH1 complexes resolved by sucrose gradient fractionation

The data in Fig. 1 showed that different relative amounts of monomeric and dimeric RC–LH1 complexes were resolved on sucrose density gradients depending on species and growth conditions, with the monomer population varying from less than 20% to 100%. This could either be an accurate reflection of the amount of monomer present in intact membranes, or it could be the case that the membrane-embedded RC–LH1 complex is exclusively dimeric, but monomerises to variable extents upon removal from the native environment using DDM. This raises the question of the sensitivity of the monomer/dimer ratio to the details of the extraction procedure.

To address this a number control experiments were carried out to examine the effects of altering the detergent concentration and other solubilisation parameters on the relative amounts of monomeric and dimeric RC–LH1 complex. One set of these experiments was carried out using *Rba. sphaeroides* strain DBCΩ, which is derived from the wild-type strain NCIB8253 and lacks the *puc* operon encoding the genes for the LH2 antenna [49]. This strain was used because the absence of LH2 avoided any contamination of the band corresponding to dimeric RC–LH1 complexes by aggregated LH2 (see above), and because it possesses a greater proportion of dimeric RC–LH1 complexes than the strain NCIB8253, allowing effects on the relative amounts of monomer and dimer to be tracked more easily.

The standard extraction protocol involved incubation of a defined concentration of membranes with 4% DDM at 4 °C for 30 min. As shown in Supplementary Fig. 1, varying the concentration of DDM between 2% and 7% had no discernable effect on the relative intensities of the lowest two intense pigmented bands corresponding to monomeric and dimeric RC–LH1 complexes, and their absorbance spectra were also unaffected (data not shown). Use of 8 or 9% DDM resulted in a smearing of bands on the gradient with a significantly smaller relative dimer population (Supplementary Fig. 1). Spectroscopic analysis of the dimer band gave a normal A_{LH1}/A_{RC} ratio (data not shown), but this ratio was notably decreased for the samples taken from the monomer band, which indicated that the detergent was disrupting the native LH1 aggregates at this concentration. Doubling the incubation time or carrying out a 30 min incubation at room temperature, both using the standard 4% DDM, also had no discernable effect on the pattern of bands or spectra of the complexes (Supplementary Fig. 1, far-right). It was therefore concluded that the relative yields of monomeric and dimeric RC–LH1 complexes fractionated on sucrose gradients were not particularly sensitive to variations in the precise conditions used for extraction from the membrane. It should also be noted that the variations in the relative populations of monomer and dimer seen for different species grown under different conditions were very reproducible, as evidenced by the standard deviations of ~±6% detailed in Table 2.

Similar experiments were carried out on *Rba. capsulatus* membranes to determine whether lowering the concentration of DDM used in the extraction would reveal the presence of dimeric RC–LH1 complexes. Varying the concentration of detergent from 6% to 0.1% produced no visible change in the pattern of bands on sucrose gradients or the spectra of the bands (Supplementary Fig. 2A,B). Concentrations of DDM lower than 0.5% achieved a very inefficient extraction of complexes from the membrane (hence the faintness of the bands in this gradient (Supplementary Fig. 2A, right)), and there was still no evidence of a dimer fraction (data not shown).

The question of whether dimeric RC–LH1 complexes could be extracted from membranes of *Rba. capsulatus* using alternative detergents or lipids was also addressed. Dimers have been isolated from *Rba. sphaeroides* using octyl β-D-glucoside (OG) [32,37] or the lipid 1,2-diheptanoyl-*sn*-glycero-3-phosphocholine (DHPC) [14], and we also tested decyl β-D-maltoside (DM) and N,N-dimethyldodecylamine N-oxide (LDAO). Supplementary Fig. 3 shows complexes extracted from *Rba. capsulatus* membranes using these detergents/lipid at concentrations between 2% and 0.5% — no dimeric RC–LH1 complexes were resolved on these gradients. Data obtained with DM was similar to that with DDM, but the other detergents did not give clean separation of LH1 and RC–LH1 monomers. With OG there was evidence of contamination of the monomer RC–LH1 fraction by LH2, and DHPC failed to separated LH2 and RC–LH1 complexes, the gradient containing smeared bands. With LDAO, spectra of bands indicated the presence of LH2 and free BChl, suggesting disaggregation of LH1. The conclusions drawn from these experiments were that DDM and DM gave the "cleanest" separation of LH2 and RC–LH1 complexes, and that alternative detergents did not enable isolation of RC–LH1 dimers from *Rba. capsulatus*.

3.4. Replacement of the Rba. sphaeroides PufX with that of Rba. capsulatus

In previous work it was shown that photosynthetic growth of *Rba. sphaeroides* was not impaired if *pufX* was replaced by the equivalent gene from *Rba. capsulatus* [41]. In the present study the effect of this replacement on the relative amount of monomeric and dimeric RC–LH1 complexes under different growth conditions was examined, employing strains either possessing or lacking the LH2 antenna. The

previous work employed LH2-deficient strains with native red/brown carotenoids that were grown under dark conditions to avoid inducing suppression mutations in non-native PufX or LH1 proteins, and to facilitate comparisons with non-photosynthetic PufX-deficient strains [41]. However, as illustrated in Fig. 1C and D, dark-grown strains with red/brown carotenoids have the drawback that the relative amount of dimer is very low when LH2 is also present, and the band expected to correspond to dimeric RC–LH1 complexes often shows contamination from aggregates of LH2. Accordingly, two equivalent sets of mutants to those described in our earlier work were constructed in the so-called "green" carotenoid background, one with and one without the LH2 antenna. The principal carotenoids in green strains are neurosporene and its hydroxy- and methoxy-derivatives [49].

Previously-constructed plasmids containing either native or chimeric *puf* operons [41] were expressed in *Rba. sphaeroides* deletion strains DPF2/G [45] and DD13/G [42], as described in Materials and methods. Both of these deletion strains are devoid of RC–LH1 complexes due to deletion of the genomic copy of the *puf* operon, and the latter is also devoid of LH2 due to a deletion of the genomic copy of the *puc* operon. The resulting transconjugant strains were named as in our previous publication [41] with upper case letters indicating the different proteins in the RC–LH1 complex and the lower case letters indicating the species (s — *sphaeroides*; c — *capsulatus*) or a deletion (d), but with the suffix "g" to denote green carotenoids and, for one set, the suffix "2" to denote the presence of LH2. For the sake of brevity, in the following the *Rba. sphaeroides* and *Rba. capsulatus* PufX proteins are referred to as PufXs and PufXc, respectively, and likewise the corresponding LH1 pigment proteins are referred to as LH1s and LH1c.

Fig. 2A (left) and C (left) shows the results of sucrose density gradient fractionation of solubilised pigment proteins from the control strain RCLH1sXs-g2, which has LH2 and an entirely *Rba. sphaeroides* RC–LH1 complex, grown under light and dark conditions, respectively. Mainly dimeric RC–LH1 complexes were extracted from light-grown cells of strain RCLH1sXs-g2 (Fig. 2A, left), whereas dark-grown cells yielded approximately equal amounts of monomer and dimer (Fig. 2C, left). Quantitative analysis of multiple intact gradients yielded values of 27% monomer and 73% dimer for light-grown cells, and 51% monomer and 49% dimer for dark-grown cells (Table 3). The PufX-deficient control strain RCLH1sXd-g2 is also shown in Fig. 2C (right) (it cannot be grown under light conditions). No dimeric RC–LH1 complexes were obtained from this strain, as expected [17,37].

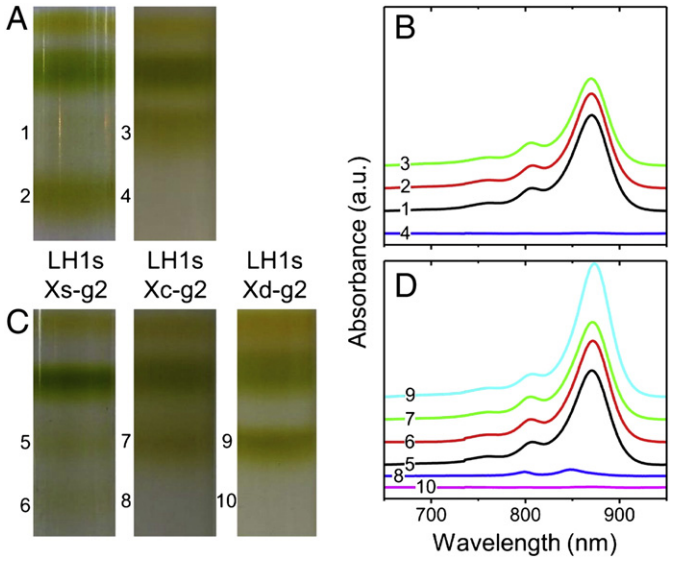

Fig. 2. Sucrose gradient fractionation and absorbance spectra of solubilised pigment proteins from strains RCLH1sXs-g2, RCLH1sXd-g2 and chimera strain RCLH1sXc-g2. (A) Fractionated pigment proteins and (B) corresponding absorbance spectra for material from cells grown under light conditions. (C) Fractionated pigment proteins and (D) corresponding absorbance spectra for material from cells grown under dark conditions. Numbers indicate the approximate position of fractions removed for spectroscopy, and resulting spectra. Strain names are given without the prefix "RC".

An equivalent analysis was also carried out on strain RCLH1sXc-g2, in which PufXs was replaced by PufXc (Fig. 2A, centre and Fig. 2C, centre). Regardless of growth conditions only monomeric RC–LH1 complexes were detected, this conclusion being based on both visual inspection and absorbance spectroscopy of intact gradients. An equivalent set of results were obtained with green strains lacking the LH2 antenna (data not shown), and strains expressing native red/brown carotenoids (data not shown); in all cases no dimeric RC–LH1 complexes were detected when PufXc replaced PufXs.

Absorbance spectra corresponding to numbered fractions from the gradients in Fig. 2A and C are shown in Fig. 2B and D, respectively. With two exceptions all the spectra indicating the presence of pigment protein had a similar line-shape, demonstrating that the monomeric RC–LH1 complexes containing the *Rba. capsulatus* PufX had the same composition as monomers and dimers containing the *Rba. sphaeroides* PufX; as shown in Table 3 there was no significant difference in the relative amounts of RC and LH1 in these complexes, as assessed through the A_{LH1}/A_{RC} ratios from several sets of gradients. One exception to this was the spectrum of PufX-deficient monomeric RC–LH1 complexes from strain RCLH1sXd-g2 (Fig. 2D, spectrum 9) which showed an elevated amount of LH1 absorbance per RC (Table 3). In strains without PufX there is a complete encirclement of LH1 around the RC in the monomeric RC–LH1 complex [14,22], requiring additional copies of the LH1 α- and β-polypeptides and associated BChls. This leads to an increase in the amount of LH1 absorbance at ~875 nm relative to RC absorbance at ~805 nm, and a significantly higher A_{LH1}/A_{RC} ratio than is observed when PufX is present in the complex. The data obtained on monomers from strain RCLH1sXd-g2 was entirely consistent with this (Fig. 2D, spectrum 9 and Table 3). The second exception was the spectrum of fraction 8 from the gradient loaded with material from strain RCLH1sXc-g2 grown under dark/semi-aerobic conditions which had a line shape indicating a (very low) level of an aggregate of LH2. There was no hint from this spectrum of the presence of RC–LH1 complexes, matching a lack of dimers in gradients loaded with complexes from light-grown cells of the same strain (Fig. 2A, centre and Fig. 2B, spectrum 4).

The capacity of the RCLH1sXc-g2 strain for photosynthetic growth was assessed alongside the controls RCLH1sXs-g2 and RCLH1sXd-g2, as described in Materials and methods. The RCLH1sXs-g2 control exhibited an approximately 10 h lag phase followed by exponential growth, and representative growth curves for six cultures are shown in Fig. 3A (black squares). The RCLH1sXd-g2 control was unable to grow over the time scale of the experiment due to the lack of a PufX in the photosystem (Fig. 3A, grey triangles), in line with previous observations. The lag phase and rate of growth for the strain RCLH1sXc-g2 (Fig. 3, light-grey circles) was not significantly different from those of the RCLH1sXs-g2 control.

Capacity for photosynthetic growth was also assessed in an equivalent set of strains with green carotenoids but lacking the LH2 antenna; these experiments were carried out at a higher light intensity to compensate for the lack of the light-harvesting capacity of LH2 (see Materials and methods). In full agreement with previous observations on equivalent strains with native red/brown carotenoids [41] the strain possessing PufXc exhibited growth that was similar to that shown by the control with PufXs (Fig. 4A, black squares and light-grey circles, respectively), within both cases strong photosynthetic growth after an adaptive lag of ~70 h. In contrast a strain lacking either PufX showed no growth over the 100 h period of the experiment (Fig. 4A, grey triangles). The findings illustrated in Figs. 3A and 4A confirmed conclusions drawn from previous work that PufXc can functionally substitute for PufXs and support photosynthetic growth [41]. It should be noted that the ~70 h lag displayed

Table 3
Quantification of photosystem components resolved through sucrose density gradient fractionation of solubilised membranes from chimera strains.

Strain	Growth	Percentage total population ± SD (n)[a]		Monomer		Dimer	
		% monomer	% dimer	A_{LH1}/A_{RC} ± SD (n)[a]	LH1 max[b] (nm)	A_{LH1}/A_{RC} ± SD (n)[a]	LH1 max[b] (nm)
RCLH1sXs-g2	Dark	51.7 ± 5.5 (8)	48.3 ± 5.5 (8)	4.06 ± 0.21 (12)	871	4.21 ± 0.17	872
	Light	27.4 ± 1.8 (6)	72.6 ± 1.8 (6)	3.91 ± 0.08 (11)	870	3.99 ± 0.32	871
RCLH1sXd-g2	Dark	100	0	5.72 ± 0.40 (14)	873	–	–
	Light	100	0	5.76 ± 0.15 (8)	874	–	–
RCLH1sXc-g2	Dark	100	0	4.19 ± 0.34 (6)	870	–	–
	Light	100	0	3.89 ± 0.06 (4)	871	–	–
RCLH1cXs-g2	Dark	100	0		–	–	–
	Light	100	0		–	–	–
RCLH1cXc-g2	Dark	100	0		–	–	
	Light	100	0	3.68 ± 0.07 (2)	875–876	–	–
RCLH1cXd-g2	Dark	100	0	5.64 ± 0.35 (4)	880	–	–
	Light	100	0	5.81 ± 0.14 (2)	879–880	–	–
RCLH1sXs-g	Dark	22.1 ± 2.39 (3)	77.9 ± 2.39 (3)	4.34 ± 0.22 (10)	871	4.71 ± 0.12 (11)	871–872
RCLH1sXd-g	Dark	100	0	6.14 ± 0.13 (10)	873	–	–
RCLH1sXc-g	Dark	100	0	4.41 ± 0.09 (3)	871	–	–
RCLH1cXs-g	Dark	100	0	3.89 ± 0.22 (7)	878	–	–
RCLH1cXc-g	Dark	100	0	4.53 ± 0.17 (4)	877–878	–	–
RCLH1cXd-g	Dark	100	0	6.30 ± 0.20 (3)	880–881	–	–

[a] n — number of gradients.
[b] Maximum of LH1 Q_y absorbance band.

by strains RCLH1sXs-g and RCLH1sXc-g was an adaptation and was not due to a genetic change, as it was still present if the strains were grown on for a second phase of photosynthetic growth following an intervening phase of growth under dark conditions (data not shown).

3.5. Heterologous expression of the Rba. capsulatus LH1 antenna in the presence of LH2

In our previous report [41] we also examined whether the *Rba. capsulatus* LH1 (LH1c) would assemble in *Rba. sphaeroides* in the presence of PufXs, PufXc or in the absence of either. Absorbance spectra of intracytoplasmic membranes from strains with red/brown carotenoids and lacking LH2 showed that an LH1 complex was indeed assembled in all three cases, but there was a significant decrease in the intensity of the LH1 absorbance band at ~875 nm relative to the RC band at ~805 nm compared to strains expressing the *Rba. sphaeroides* LH1 (LH1s) [41]. Organisation of RCs and LH1c complexes in these strains was not examined, but in principle they could contain lowered levels of "normal" monomeric or dimeric RC–LH1 complexes together with naked RCs, or RC–LH1 complexes with a reduced complement of LH1c, either as a uniform population or a distribution of sizes.

In the present work, LH1c was expressed in strains containing LH2 and with green carotenoids. Three strains were constructed, possessing PufXs (RCLH1cXs-g2), PufXc (RCLH1cXc-g2) or lacking a PufX (RCLH1cXd-g2). Photosynthetic growth of these strains was compared with that of the controls RCLH1sXs-g2 and RCLH1sXd-g2 that

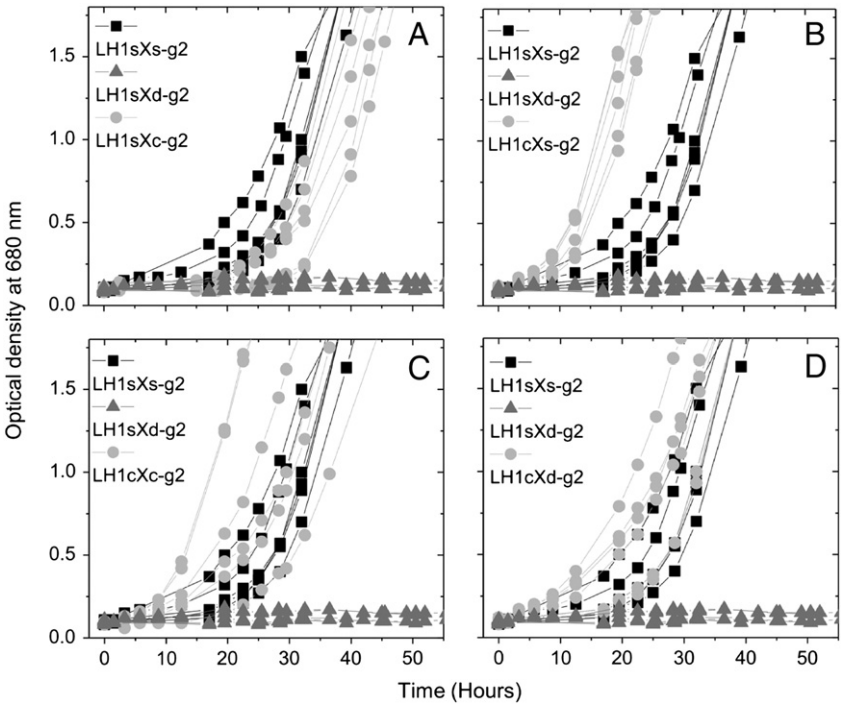

Fig. 3. Growth under photosynthetic conditions for strains with LH2. Six cultures were grown in parallel for each strain and each panel includes data for PufXs-containing strain RCLH1sXs-g2 (black squares) and PufX-deficient strain RCLH1sXd-g2 (grey triangles, compared with data (light-grey circles) for strain (A) RCLH1sXc-g2, (B) RCLH1cXs-g2, (C) RCLH1cXc-g2, (D) RCLH1cXd-g2.

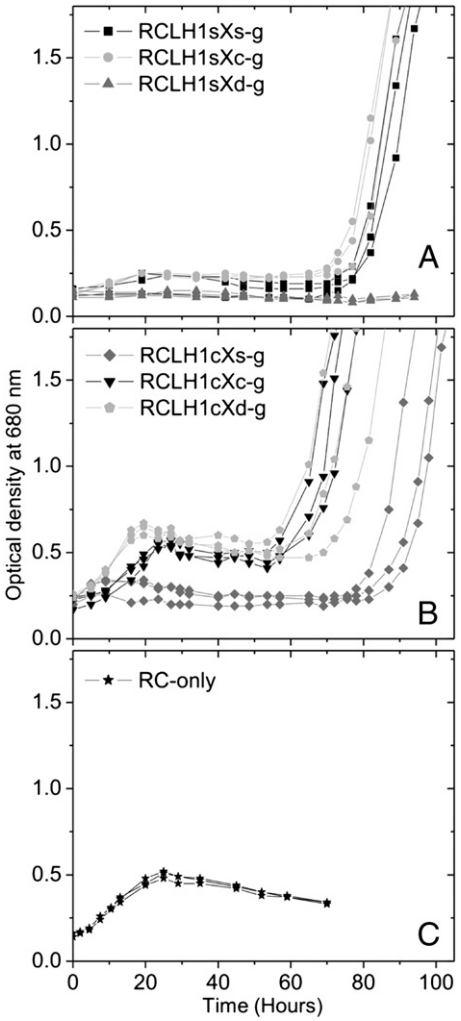

Fig. 4. Growth under high light photosynthetic conditions for strains lacking LH2. Four cultures were grown in parallel for each strain. (A) Growth of strains RCLH1sXs-g (black squares), RCLH1sXs-g (light-grey circles) and RCLH1sXd-g (grey triangles). (B) Growth of strains RCLH1cXs-g (grey diamonds), RCLH1cXc-g (black triangles) and RCLH1cXd-g (light-grey pentagons). (C) Growth of a strain lacking both LH1 and LH2 (black stars).

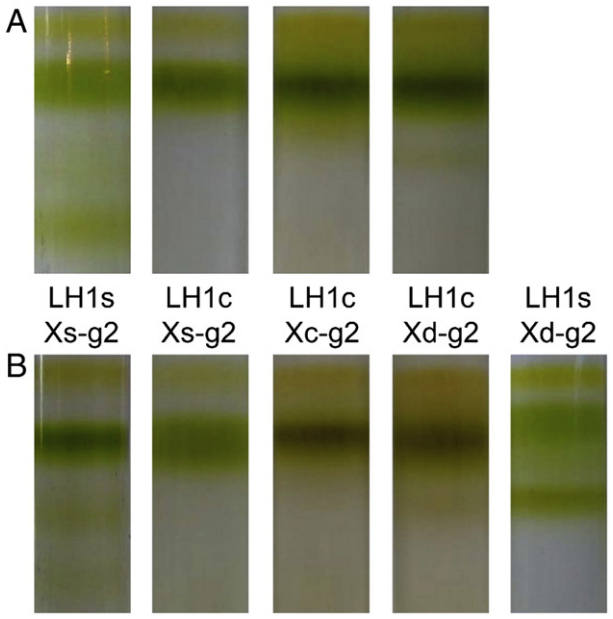

Fig. 5. Sucrose gradient fractionation of solubilised pigment proteins from LH2-containing *Rba. sphaeroides* strains with native or altered RC-LH1 complexes. (A) Fractionated pigment proteins from cells grown under light conditions. (B) Fractionated pigment proteins from cells grown under dark conditions. Strain names are given without the prefix "RC".

contained LH1s (Fig. 3B–D). All three strains expressing LH1c were capable of photosynthetic growth, and for strains RCLH1cXc-g2 (Fig. 3C, light-grey circles) and RCLH1cXd-g2 (Fig. 3D, light-grey circles) the characteristics of this growth were similar to those displayed by the RCLH1sXs-g2 control (black squares). In the case of strain RCLH1cXs-g2 (Fig. 3B, light-grey circles) its growth appeared to be consistently significantly faster than that of the RCLH1sXs-g2 control (black squares).

The results of fractionating the solubilised membrane proteins originating from photosynthetically-grown cells of these strains are shown in Fig. 5A. Surprisingly, given their capacity for photosynthetic growth, the RCLH1cXc-g2 and RCLH1cXd-g2 strains had only a very small amount of monomeric RC–LH1 complexes and no dimeric complexes (gradients labelled LH1cXc and LH1cXd, respectively) whereas no RC–LH1 complexes of either sort were detected in the case of the RCLH1cXs-g2 strain (gradient labelled LH1cXs). Similar results were observed when the same strains were grown under dark/semi-aerobic growth conditions (Fig. 5B). The spectrum of the small amount of PufXc-containing monomeric RC–LH1 complex that was resolved on these gradients (not shown) was similar to that of PufXs-containing monomers in terms of line-shape and A_{LH1}/A_{RC} ratio (Table 3). Furthermore the spectra of the small amount of monomers assembled in the RCLH1cXd strain had a high ratio of A_{LH1}/A_{RC} (>5.5) typical of a PufX-deficient RC–LH1 complex (Table 3).

These findings called into question whether the photosynthetic growth observed for these LH2-containing strains expressing the *Rba. capsulatus* LH1 genes could be attributed to the strongly depressed levels of chimeric RC–LH1 complex present, particularly for strain RCLH1cXs-g2 where no RC–LH1 complexes could be detected. Given that the level of expression of the *Rba. sphaeroides* RC should not be affected by changes to the complement of PufX and/or LH1 proteins [49], and appreciable levels of RC must have been present in these strains to achieve photosynthetic growth, this led to the conclusion that it was more likely that the photosynthetic growth shown in Fig. 3B–D was attributable to free RCs interacting directly with LH2, with the small amounts of RC–LH1 complex in strains RCLH1cXc-g2 and RCLH1cXd-g2 playing only a minor role. Such LH1-independent growth is well documented, including in strains of *Rba. sphaeroides* that also lack PufX [50]. A band corresponding to LH1-free RCs was not seen on the gradients shown in Fig. 5 because the position that RCs migrate to on such gradients is similar to that of LH2, and their largely coincident absorbance spectra would make a minor population of RCs difficult to detect in the presence of an excess of LH2. This point is returned to below.

3.6. Heterologous expression of the Rba. capsulatus LH1 antenna in the absence of LH2

To investigate further whether the LH1c-containing strains had functional RC–LH1 complexes and/or a population of free RCs an analysis was carried out on an equivalent set of strains expressing LH1c but lacking LH2. These strains were denoted RCLH1cXs-g, RCLH1cXc-g and RCLH1cXd-g, and their properties were compared with equivalent LH2-deficient control strains RCLH1sXs-g and RCLH1sXd-g. The spectra of cells and membranes from the strains possessing the LH1c protein showed a decreased LH1 absorbance at ~875 nm relative to RC absorbance ~805 nm (by a factor of approximately 50% — data not shown), consistent with our earlier study which was also carried out on LH2-deficient strains but with red/brown carotenoids [41].

The results of sucrose density gradient fractionation of solubilised pigment proteins from dark-grown cells are shown in Fig. 6A. Gradients for the three LH2-deficient strains expressing LH1c (Fig. 6A, centre) had an additional purple band (numbered 1–3) at a position between the green band at the top of the gradient corresponding to free carotenoid and the lower khaki band due to monomeric RC–LH1 complexes. This purple band was not evident in gradients loaded with material from either control strain containing LH1s (Fig. 6A, left and second from right). DDM-solubilised RCs from a *Rba. sphaeroides* strain devoid of both LH2 and LH1 (Fig. 6A, right, band 4) were found to migrate to the same position as the purple bands seen in the gradients fractionating proteins from strains expressing LH1c (Fig. 6A, centre). Samples of purple bands 1–4 were removed, spectra recorded, corrected for background scatter between 650 and 950 nm and normalized to the same amplitude of the band at ~805 nm (Fig. 6B). All four spectra had the line shape expected for the RC, with possible contamination by a small amount of LH1 for the gradients loaded with pigment proteins from strains RCLH1cXs-g (band/spectrum 1) and RCLH1cXc-g (band/spectrum 2), evidenced by a very small additional absorbance at ~875 nm. Thus it was concluded that membranes from the strains expressing the LH1c had a sizeable population of free RCs; as discussed above, in sucrose gradient analysis of strains possessing LH2 this population would be masked by LH2 which migrates to the same position on the gradient (compare Fig. 6A with Fig. 5).

Turning to the remaining pigmented bands in Fig. 6A, the control strain RCLH1sXs-g had a high proportion of dimeric RC–LH1 complexes (Fig. 6A, bands 5 and 6) whereas the PufX-deficient control strain, RCLH1sXd-g, had only monomeric RC–LH1 core complexes, as expected (Fig. 6A, band 10). The percentage of dimer from a quantitative analysis of multiple intact gradients was 78% for RCLH1sXs-g and 0% for RCLH1sXd-g (Table 3). In all three gradients loaded with material from strains expressing LH1c there was no indication of the presence of dimeric RC–LH1 core complexes from a visual inspection of the gradients (Fig. 6A, centre), and this was confirmed by a spectroscopic analysis of intact gradients (data not shown).

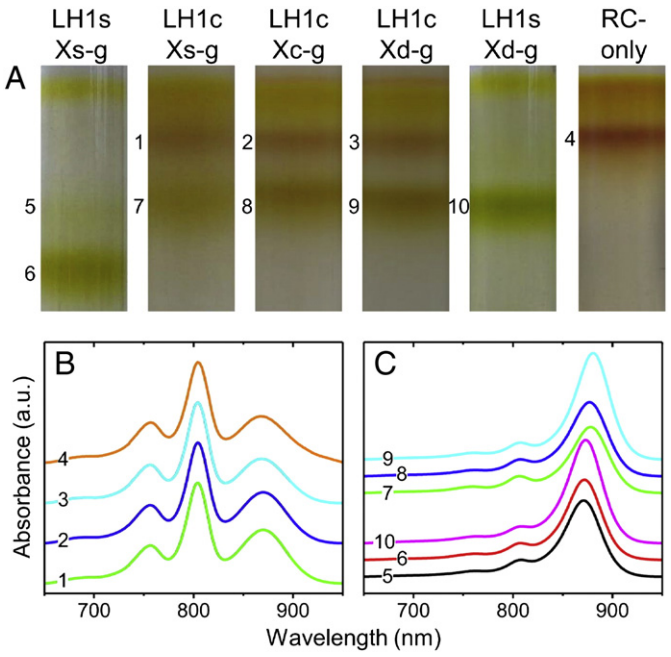

Fig. 6. Sucrose gradient fractionation and absorbance spectra of solubilised pigment proteins from LH2-deficient *Rba. sphaeroides* strains with native or altered RC-LH1 complexes. (A) Fractionated pigment proteins from cells grown under dark conditions. (B) Corresponding absorbance spectra for pigmented bands 1–4. (C) Corresponding absorbance spectra for pigmented bands 5–10. Numbers indicate the approximate position of fractions removed for spectroscopy, and resulting spectra. Strain names are given without the prefix "RC".

Samples of RC–LH1 complexes were removed from the gradients at the positions shown by the numbers in Fig. 6A and absorbance spectra recorded (Fig. 6C). Spectra of monomeric RC–LH1 complexes containing LH1c (Fig. 6C, bands 7–9) showed a red shift in the maximum of the LH1 absorbance band of between 7 and 10 nm, relative to the position of this band in the spectrum of RC–LH1 complexes containing LH1s (Fig. 6C, bands 5, 6 and 10). This observation correlated with the red shift of this band seen for the *Rba. capsulatus* RC–LH1 complex isolated from wild-type strain Kb-1 (Fig. 1B and D). Aside from the red shift of the LH1 absorbance band, the spectrum of monomers from strains RCLH1cXs-g and RCLH1cXc-g (Fig. 6C, spectra 7 and 8, respectively) was similar to that of monomers and dimers from the control strain RCLH1sXs-g (Fig. 6C, spectrum 5), suggesting a uniform composition for these complexes with a RC surrounded by an incomplete ring of LH1 pigment protein, closure of the ring being prevented by either PufXs or PufXc. Values of A_{LH1}/A_{RC} for these complexes determined from analysis of multiple intact gradients are shown in Table 3. The spectrum of the monomeric RC–LH1 complexes from strain RCLH1cXd-g (Fig. 6C, spectrum 9) was similar to that of monomers from strain RCLH1sXd-g (Fig. 6C, spectrum 10), showing an increased amount of LH1 absorbance per unit RC absorbance (quantified in Table 3). The simplest interpretation of this was that removal of PufX caused complete encirclement of the RC by LH1c in a manner similar to that obtained with LH1s.

Another striking feature of the three gradients loaded with material from strains expressing LH1c (Fig. 6A, centre) was the high concentration of carotenoid at the top of the gradient relative to the two controls expressing LH1s (Fig. 6A, left and second from right). This accumulation of carotenoid was also observed for the gradient loaded with material from the RC-only strain (Fig. 6A, right). In contrast there was no evidence of accumulation of free bacteriochlorin pigments in these strains with strongly reduced photosystems.

The capacity for photosynthetic growth of the LH2-deficient strains expressing LH1c was examined. Previous work on equivalent strains with native red/brown carotenoids reported an unusual biphasic photosynthetic growth at high light intensity for the strains with PufXc or no PufX, but not for the strain with PufXs [41]. Fig. 4B shows photosynthetic growth of three replicate cultures of strains RCLH1cXs-g (grey diamonds), RCLH1cXc-g (black triangles) and RCLH1cXd-g (light-grey pentagons). Broadly consistent with our previous study, strains RCLH1cXc-g and RCLH1cXd-g both showed an initial phase of growth with no lag, followed by a levelling-off of the OD of the culture at a value of 0.5–0.7 and then a strong phase of growth starting around 50 h. In our previous work this initial phase was not attributed, although it was pointed out that it had similarities to the weak photosynthetic growth of a so-called RC-only strain that lacks both LH1 and LH2 [41]. However, the analysis described in Fig. 6 showed that strains RCLH1cXc-g and RCLH1cXd-g both contained a sizeable population of antenna-free RCs in addition to monomeric RC–LH1 complexes, and so the initial phase of photosynthetic growth exhibited by these strains can now more firmly be attributed to growth facilitated by free RCs. Growth of an antenna-deficient strain of *Rba. sphaeroides* with green carotenoids is shown for comparison in Fig. 4C; growth of this "RC-only" strain proceeded with no lag but levelled off when the culture reached an OD of around 0.5, gradually declining thereafter. This failure of RC-only cultures to achieve high culture densities has previously been attributed to their limited light-harvesting capacity [41]. Comparison of Fig. 4C and B demonstrates that the phase of strong exponential growth starting at t = 50 h seen for strains RCLH1sXs-g and RCLH1cXs-g can be attributed to their complement of RC–LH1 complexes, as this was not seen for the antenna-deficient control strain (Fig. 4C).

Also consistent with our earlier report, growth of strain RCLH1cXs-g did not shown an initial phase of photosynthetic growth that is attributable to antenna-free RCs. This was despite the fact that free RCs were present in this strain at levels comparable to those seen

in strains RCLH1cXc-g and RCLH1cXd-g (Fig. 6A). Possible reasons for this difference are considered in the discussion. Instead, strain RCLH1cXs-g showed the sort of photosynthetic growth seen in the RCLH1sXs-g and RCLH1sXc-g strains (Fig. 4A), with an exponential phase attributable to RC–LH1 complexes that followed a long adaptive lag of ~70 h.

3.7. Exploring the photosystem components present in other Rhodobacter species

To cast light on whether the dimers seen in *Rba. sphaeroides*, *azotoformans* and *blasticus* represent an atypical or typical structural arrangement, and whether greater structural variety exists within the genus *Rhodobacter*, RC–LH1 complexes from two less well-characterised species were examined. Isolates of *Rba. vinaykumarii* and *Rba. changlensis* were grown under both dark and light conditions, as described in Materials and methods. Pigment-protein complexes were solubilised from intracytoplasmic membranes and fractionated on sucrose density gradients by ultracentrifugation.

The results of this analysis are summarised in Fig. 7, with data for *Rba. sphaeroides* shown for comparison. The gradients for all three species exhibited an upper intense pigmented band corresponding to LH2 (Fig. 7A and C for light- and dark-grown cells, respectively) and a lower band corresponding to monomeric RC–LH1 complexes. The twin LH2 bands seen in gradients loaded with material from *Rba. sphaeroides* were also seen for the other species in Fig. 7, but with some variation in the relative intensities of the two bands, particularly for dark-grown *Rba. changlensis* (Fig. 7C, right).

Both light-grown and dark-grown *Rba. vinaykumarii* had a band corresponding to monomeric RC–LH1 complexes (Fig. 7A, left and 7 C, left, respectively). The spectra of monomers (Fig. 7B, spectrum 1 and 7D, spectrum 7) was similar to that of *Rba. sphaeroides* monomers (Fig. 7B, spectrum 3 and 7D, spectrum 9), but with a ~2 nm blue shift of the LH1 absorbance band (Table 2). Average values of A_{LH1}/A_{RC} were slightly lower than those of the equivalent *Rba. sphaeroides* complexes, but this difference was not significant for dark-grown cells and of marginal significance for light-grown cells (Table 2). No dimers could be detected for light-grown (Fig. 7A, left) or dark-grown (Fig. 7C, left) *Rba. vinaykumarii*, spectra of aliquots extracted from gradients at positions 2 and 8 being featureless (Fig. 7B, spectrum 2 and Fig. 7D, spectrum 8).

Rba. changlensis showed clear evidence for the presence of dimers in both light-grown and dark-grown cells, (Fig. 7A and C, right), with absorbance spectra (Fig. 7B, spectrum 6 and 7D, spectrum 12) and A_{LH1}/A_{RC} ratios (Table 2) similar to those for the corresponding complex from light-grown *Rba. sphaeroides* (Fig. 7C, spectrum 4). Unlike in *Rba. sphaeroides* the dimer band from dark-grown cells was not contaminated with LH2 (Fig. 7D, spectrum 12). The *Rba. changlensis* RC–LH1 complex was primarily monomeric in dark-grown cells (72%) shifting to a more even distribution in light-grown cells (59% monomer, 41% dimer), in line with the trend seen for both *Rba. sphaeroides* and *Rba. azotoformans* (Table 2).

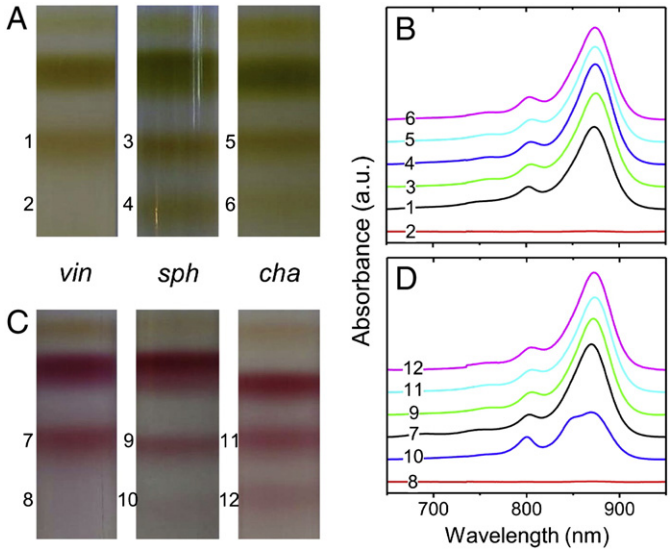

Fig. 7. Sucrose gradient fractionation of solubilised pigment proteins from *Rba. vinaykumarii*, *Rba. sphaeroides* and *Rba. changlensis*. (A) Fractionated pigment proteins and (B) corresponding absorbance spectra from light-grown cells. (C) Fractionated pigment proteins and (D) corresponding absorbance spectra from dark-grown cells. Numbers indicate the approximate position of fractions removed for spectroscopy, and resulting spectra. Key: *vin*— *Rba. vinaykumarii*, *sph*— *Rba. sphaeroides*, *cha*— *Rba. changlensis*.

4. Discussion

4.1. Monomeric and dimeric RC–LH1 complexes in vivo and in vitro

As outlined in the Introduction, extraction of RC–LH1 complexes from *Rba. sphaeroides* membranes consistently produces a mixture of monomeric and dimeric forms, producing two discrete bands when solubilised RC–LH1 complexes are fractionated on sucrose density gradients [17,21,32,37,46]. An open question is the extent to which the distribution between monomeric and dimeric RC–LH1 complexes isolated in this way is an accurate reflection of the distribution in the membrane, as side-by-side comparisons of quantitative data from AFM and sucrose density gradients have not been carried out. As one aim of the present work was to look for evidence of dimeric RC–LH1 complexes in other species or engineered strains, particular attention was paid to how the precise conditions of DDM extraction of membranes affected the profile of isolated complexes.

One point that emerged from the data shown in Figs. 1, 2, 5–7, Supplementary Fig. 1 and Tables 2 and 3 is that the relative amounts of monomer and dimer obtained for a particular *Rba. sphaeroides* strain grown under particular conditions showed good reproducibility across several sets of bacterial cultures, DDM extractions and sucrose gradients. In control experiments carried out on a number of strains, one of which is shown in Supplementary Fig. 1, halving or near-doubling the concentration of DDM used in the extraction had no significant effect on the relative amount of monomer and dimer, nor did doubling the time of the detergent extraction, or carrying it out at room temperature. If the monomer population arises from dissociation of dimers during the extraction then one might have expected the relative amount of monomer to increase with increases in detergent concentration, or extraction time or temperature, but this was not observed.

A second point to emerge from the data on *Rba. sphaeroides* was that there was considerable (but reproducible) variation in the relative amount of monomer and dimer depending on the strain studied and growth conditions employed. So, for example, the dimer yield was 0% for dark-grown wild-type, 37% for light-grown wild-type, 49% for the dark-grown green RCLH1sXs-g2 strain, and 73% for the light-grown green RCLH1sXs-g2 strain (Tables 2 and 3). When LH2 was removed, in strain RCLH1sXs-g, the dimer yield was 78% in dark-grown cells; under these conditions the *Rba. sphaeroides* is expected to assemble dimer-rich tubular membranes [51]. These observations either mean that the amount of dimer assembled in the membrane is variable, with a tendency for higher relative populations in light-grown cells where the photosynthetic apparatus is active, or that the stability of the dimer is different in the different types of strain/growth conditions, which would imply differences in composition and/or structure. Contributory factors could be differences in carotenoid type or lipid profile under different growth conditions. A similar dependence of dimer yield on growth conditions was seen for *Rba. azotoformans* (Fig. 1 and Table 2), where a higher yield was

obtained in light-grown cells (83%) then dark-grown cells (37%), and to a less marked extent in *Rba. changlensis* (Fig. 7 in Table 2) where the equivalent values were 41% and 29%, respectively.

To summarise, it is not clear whether the monomers observed upon fractionation of DDM-solubilised pigment proteins on sucrose gradients are dissociated dimers, but given published evidence that the monomeric form is found in intact membranes, the insensitivity of the monomer yield to extraction conditions and the reproducible variations in monomer/dimer yields in different strains of *Rba. sphaeroides* grown under different conditions, it seems more likely that the results obtained with the sucrose gradients are a good reflection of the relative amounts of monomeric and dimeric RC–LH1 complexes in the membrane.

4.2. The composition of the RC–LH1 complexes

The data summarised in Tables 2 and 3 analyse the absorbance spectra of a range of monomeric and dimeric RC–LH1 complexes, presenting A_{LH1}/A_{RC} ratios obtained by dividing the absorbance at the maximum of the LH1 Q_y band (which was between 869 and 881 nm depending on species or mutation) by the absorbance at the maximum of the RC band at around 805 nm. For monomers or dimers from PufX-containing strains this ratio had average values between 3.7 and 4.9. Although there is a large spread between these limits, there were no obvious statistically-significant trends between monomers and dimers or between particular types of strain that might lead one to suspect a real difference in the aggregation state of LH1 surrounding the RC. This ratio was calculated as a simple indicator of core complex composition, and to give a convenient way of quantifying typical variability in the absorbance spectra obtained for a particular complex. As such it did not take into account variations in width of the LH1 absorbance band or differences in its overlap with the underlying absorbance band of the RC. The only clear trend that can be pointed to was the significant increase in A_{LH1}/A_{RC} ratio seen in PufX-deficient monomers (Figs. 2D and 6C), where values between 5.6 and 6.3 were obtained due to the additional BChls and associated proteins that close the ring of LH1 around the RC in the absence of PufX. The fact that such an increase in A_{LH1}/A_{RC} was not seen when, for example, PufXs was replaced by PufXc, allows the inference that the non-native PufX is incorporated into the RC–LH1 complex in place of the native protein.

What do the data summarised in Tables 2 and 3 mean in terms of the composition of the monomeric RC–LH1 complex? The number of pairs of LH1 α- and β-polypeptides surrounding each RC has been variously estimated to be 13 for *Rba. blasticus*[18] and 12 or 14 for *Rba. sphaeroides*[13,15,17], with 14 the currently favoured number in the latter case [15]. These estimates are based on pigment analyses and a variety of low-resolution structural data (see Holden-Dye et al. [21] for a review). For *Rba. veldkampii*, which does not assemble dimers, it has been proposed that the RC is surrounded by 15 α/β pairs [20]. *Rba. veldkampii* did not form part of the present study, but an absorbance spectrum of monomers has been published [20] and it is possible to calculate a A_{LH1}/A_{RC} ratio of around 4.8 from this, consistent with the upper end of the range of values for monomers obtained in the present study. As discussed in detail by Holden-Dye et al. [21], estimates of ratios of LH1 BChls per RC for RC–LH1 complexes with and without PufX vary considerably, with the only point of agreement being that this ratio increases when PufX is removed. Given this, the most that can be said is that it is likely that PufX-containing RC–LH1 monomers contain between 13 and 15 LH1α/β pairs, with perhaps some variation between species.

4.3. Is the Rba. azotoformans or Rba. capsulatus RC–LH1 complex dimeric?

The data shown in Fig. 1 demonstrate that the *Rba. azotoformans* RC–LH1 complex assembles in the dimeric form. In fact the PufL, PufM and PufX proteins from *Rba. azotoformans* exhibit a high degree of identity with those from *Rba. sphaeroides* (Table 1), which would suggest that the two species are closely related. This has been borne out by phylogenetic trees based on genes for 16S rRNA, the RC PufM protein or *c*-type cytochromes that consistently group *Rba. sphaeroides* and *Rba. azotoformans* closely together [38,52–54].

To our knowledge there have been no published accounts of attempts to detect dimeric RC–LH1 complexes in *Rba. capsulatus*. The data described in Fig. 1 indicate that when isolated from intracytoplasmic membranes using DDM the *Rba. capsulatus* RC–LH1 complex is 100% monomeric, with no hint of a dimeric form. This was the case for both light-grown and dark-grown cells. Taken together with the observation that dimers were not obtained when PufXs was replaced by PufXc (Fig. 2), or when PufXs was combined with LH1c (Figs. 5 and 6), we conclude that it seems unlikely that the *Rba. capsulatus* RC–LH1 complex assembles in a dimeric form, but rather it has the monomeric form as observed in intact membranes from *Rba. veldkampii*. Alternately, if dimers are assembled in the membrane in *Rba. capsulatus* then they must be substantially less stable on detergent extraction than their *Rba. sphaeroides* counterparts. For the reasons outlined above we currently favour the first of these interpretations.

Is there circumstantial evidence concerning whether dimeric RC–LH1 complexes are present or absent in *Rba. capsulatus*? One striking finding with *Rba. sphaeroides* is that deletion of the LH2 antenna changes the architecture of the intracytoplasmic membrane from vesicular to tubular [51,55,56], and very convincing evidence has been published that this highly-ordered tubular architecture is a direct consequence of the bent structure of the RC–LH1 dimer [57]. If the *Rba. capsulatus* RC–LH1 complex were dimeric then one might expect LH2-deficient strains of *Rba. capsulatus* to similarly possess tubular membranes. To our knowledge there are no published data on the structure of intracytoplasmic membranes in such a strain, but in a review of membrane architecture in photosynthetic bacteria, Drews commented that "Recent studies with *Rba. capsulatus* mutants in which the *puc* operon was completely deleted showed vesicles of irregular size, but no tubules (J.R. Golecki and G. Drews, unpublished)" [58]. Such a difference in membrane architecture between LH2-deficient strains of *Rba. sphaeroides* and *Rba. capsulatus* would be consistent with the RC–LH1 complex being dimeric (and tube forming) in the former but not in the latter.

4.4. Insights from other species

The yields of extracted monomer and dimer were also examined in two recently characterised species of *Rhodobacter*. *Rba. vinaykumarii* was isolated from seawater on the coast of northern India and is salt-tolerant, showing growth at up to 10% NaCl [40]. *Rba. changlensis* was isolated from snow from Changla Pass in the Indian Himalayas and is cold-tolerant, showing growth down to 5 °C [39]. Both have vesicular membranes, and have absorbance spectra consistent with the presence of LH1, LH2, BChl *a* and spheroidene/spheroidenone carotenoids [39,40]. *Rba. changlensis* exhibited a dimer band when pigment proteins were fractionated on sucrose gradients (Fig. 7A,C), the amount of dimer being intermediate between that seen in *Rba. sphaeroides* and *Rba. azotoformans* in dark-grown cells, and similar to that seen in *Rba. sphaeroides* in light-grown cells (Table 2). In contrast no dimers were detectable in the case of *Rba. vinaykumarii* (Fig. 7A,C), similar to the result obtained with *Rba. capsulatus* (Fig. 1A,C) and reported elsewhere for *Rba. veldkampii* [19,20,48]. The spectra of monomers from *Rba. vinaykumarii*, *capsulatus*, *changlensis* and *azotoformans*, and of dimers from the latter two, were similar to that of their counterparts from *Rba. sphaeroides*, suggesting a similar composition of a RC surrounded by ~14 (±1) pairs of LH1 BChls (Table 3).

The phenotypes observed for *Rba. vinaykumarii* and *Rba. changlensis* were interesting given what is known about phylogenetic relationships between the twelve currently identified species of *Rhodobacter* based

on 16s rRNA gene sequences [59]. These show that *Rba. changlensis* groups with *Rba. azotoformans and Rba. sphaeroides*, which also assemble dimers, whereas *Rba. vinaykumarii* groups more closely with *Rba. veldkampii* and *Rba. capsulatus*, which fail to yield dimers on sucrose gradients. This said, the latter group also includes *Rba. blasticus*, which is also known to assemble dimers, and so this division between strains that do and do not show evidence of the presence of dimers is not absolute. It has been reported, however, that *Rba. blasticus* has lamellar-structure photosynthetic membranes [60,61] unlike all other characterised species of *Rhodobacter*, which could imply that the dimeric RC–LH1 complexes assembled in this species do not have a bent architecture such as that observed for *Rba. sphaeroides*[57], as pointed out previously [46]. More insightful might be phylogenetic trees based on sequences from the *puf* operon, but unfortunately such sequence information is currently patchy, being known in full only for *Rba. sphaeroides* and *capsulatus*, and in part for *Rba. blasticus, azotoformans* and *veldkampii.* More sequence information on the LH1 polypeptides in particular would be valuable, as it is likely that these proteins are involved in the molecular interactions that determine whether or not a dimeric form of the RC–LH1 complex is assembled (see below).

4.5. Dimer motifs

In a number of publications, attempts have been made to use alignments of PufX sequences to identify patterns of amino acids that could account for the fact that dimeric RC–LH1 complexes assemble in *Rba. sphaeroides* but not in *Rba. veldkampii*, so-called "dimerization motifs". Two of these [19,48] have relied on the assumption that the RC–LH1 complexes of *Rba. azotoformans* and *capsulatus* are dimeric, and from the data described above we conclude that the *Rba. azotoformans* does indeed assemble dimeric RC–LH1 complexes, but the data do not support the assumption that the *Rba. capsulatus* RC–LH1 complex is dimeric, undermining the logic of these proposed dimerisation motifs.

A third proposal [20,62] is that dimerisation of the *Rba. sphaeroides* PufX, and hence the entire RC–LH1 complex, is facilitated by a GxxxG helix dimerisation motif of the type found in glycophorin A [63,64]. Two adjacent possible motifs are present in the *Rba. sphaeroides* PufX, in the sequence $G^{31}xxxG^{35}xxxG^{39}$, whereas in monomer-containing *Rba. veldkampii* the equivalent sequence is GxxxVxxxG [20]. In a recent report we have shown that Leu substitutions at Gly^{31}, Gly^{35} and Gly^{39} have no effect on the relative amounts of *Rba. sphaeroides* monomers and dimers resolved on sucrose gradients [46], in contrast to expectations from mutagenesis studies of glycophorin A [63,64]. This proposal is further argued against through the data obtained in the present work, as the relevant sequence in dimer-containing *Rba. azotoformans* is GxxxAxxxG.

4.6. PufXc can fulfill some, but not all, of the functions of PufXs

In our previous study of chimeric RC–LH1 complexes [41], employing LH2-deficient strains expressing native red/brown carotenoids, it was established that membrane-embedded RC–LH1 complexes from a strain expressing PufXc had an absorbance spectrum consistent with the presence of PufX-containing RC–LH1 complexes, and inconsistent with the presence of PufX-deficient complexes (as assessed from the A_{LH1}/A_{RC} ratio). Photosynthetic growth of *Rba. sphaeroides* was largely unaffected by replacement of PufXs by PufXc, and so it was concluded that PufXc was incorporated into chimeric RC–LH1 complexes that had a normal complement of LH1 BChls per RC and were functionally active. This was despite the fact that PufXc shares only 23% sequence identity with PufXs.

In the present work these findings were reproduced in equivalent strains expressing green carotenoids and containing LH2 (Figs. 2 and 3A). In addition, sucrose gradient fractionation gave more detailed insights into the organisation of the chimeric RC–LH1 complexes, revealing a population of monomers but no evidence of dimers (Fig. 2A and C). Following the discussion above the more likely interpretation of this is that only the monomeric form of this chimeric RC–LH1 complex is assembled in membranes of this strain during cell growth. Similar results were obtained with green strains lacking LH2; PufXc-containing RC–LH1 complexes supported photosynthetic growth in a manner similar to those containing PufXs (Fig. 4A), but no dimeric RC–LH1 complexes were detected on sucrose gradients when PufXc was present (not shown). It would appear, therefore, that PufXc is able to assemble into the *Rba. sphaeroides* RC–LH1 complex to yield a monomer that has a similar number of LH1 BChls per RC as native monomers, and is competent in supporting photosynthetic growth, but it does not possess the ability to promote dimer formation. This correlates with the finding that dimeric RC–LH1 complexes could also not be isolated from wild-type *Rba. capsulatus* (Fig. 1).

4.7. Insights from heterologous expression of LH1c

In our previous study we also expressed LH1c in LH1s and LH2-deficient strains of *Rba. sphaeroides* with red/brown carotenoids and having PufXs, PufXc or no PufX [41]. A striking finding was that the level of expression of LH1c was around 50% of that of the native LH1s, as assessed from the relative intensity of LH1 and RC absorbance in spectra of cells and membranes [41]. This result was reproduced in the present study employing equivalent strains with green carotenoids (data not shown), and sucrose gradient fractionation was used to look at the composition of the pigment proteins assembled in these strains (Fig. 6). Separate populations of LH1-free RCs and monomeric RC–LH1 complexes were resolved in all three strains expressing LH1c, but no dimers were detected on these gradients. The monomeric RC–LH1 complexes containing LH1c and either PufXs or PufXc had an A_{LH1}/A_{RC} ratio similar to that of native *Rba. sphaeroides* and *Rba. capsulatus* monomers. This suggests that the assembly of a reduced number of chimeric RC–LH1 complexes of "normal" composition was more favourable than the formation of partially-assembled RC–LH1 complexes with a distribution of A_{LH1}/A_{RC} ratios, or independent populations of LH1-free RCs and RC-free LH1 complexes. The most obvious interpretation of this is that the fully assembled RC–LH1 complex, comprising a RC, PufX and ring of ~14 pairs of α/β-polypeptides, represents a minimum energy structure that assembles preferentially even when components are taken from different species. The monomers isolated from strain RCLH1cXd-g had the elevated A_{LH1}/A_{RC} ratio characteristic of PufX-deficient monomers obtained in strains expressing LH1s, and are considered further in the next section.

No dimeric RC–LH1 complexes were observed in the strain expressing a combination of LH1c and PufXs, in contrast to the situation in strains expressing LH1s and PufXs (Fig. 6A). This reinforces the point made above, that the presence of dimers in *Rba. sphaeroides* is not dictated solely by PufXs, but rather is determined by a combination of PufXs and LH1s. If either or both are replaced by the *Rba. capsulatus* variant then no dimers are assembled.

The reason for the lowered level of LH1c expression in *Rba. sphaeroides* was not investigated. However it is worth noting that, unlike in *Rba. sphaeroides*[42], assembly of LH1c in *Rba. capsulatus* shows a dependence on the assembly of normal levels of the RC, strains with mutations in RC structural genes that depress the level of RC expression also exhibiting lowered levels of LH1 [28,65]. Thus one possibility is that the *Rba. sphaeroides* RC is able to only partially substitute for the *Rba. capsulatus* RC during heterologous expression of LH1c, fulfilling some, but not all, of the molecular interactions involved.

When LH2 was present photosynthetic growth was seen for all three strains expressing LH1c (Fig. 3B–D), but to our surprise only very low levels of monomeric RC–LH1 complexes were detected for strains RCLH1cXd-g2 and RCLH1cXc-g2 (the latter only in light-grown cells — Fig. 5), and no RC–LH1 complexes could be detected for strain RCLH1cXs-g2. As experiments with the equivalent strains lacking LH2 had shown evidence of substantial populations of

antenna-free RCs (Fig. 6A,B), the photosynthetic growth seen in the LH2-containing strains was attributed to the action of LH1-free RCs that are fed with additional excitation energy directly by LH2. Such photosynthetic growth of *Rba. sphaeroides* strains completely lacking LH1 has been reported previously [50]. At present it is not clear why so little LH1c was assembled when LH2 was also present, but it could suggest inhibition of LH1c assembly by one or more components of LH2 or associated assembly factors. In support of this, Jaschke and co-workers in experiments with *Rba. capsulatus* have observed interference in the assembly of LH1 by LH2 polypeptides when an LH2 assembly factor known as PucC is absent [66], and so one possibility is that the equivalent *Rba. sphaeroides* PucC is not able to prevent inhibition of the assembly of a non-native LH1 by the native LH2. Another possibility is that there is some degree of competition between assembly of the *Rba. sphaeroides* LH2 and LH1c, with assembly of the latter being unable to compete with assembly of high levels of the native LH2. In support of this, Adams and co-workers have recently reported lowered rates of LH2 assembly in a strain of *Rba. sphaeroides* in which assembly of LH1 is enhanced through removal of PufX [33].

In the present study the data on photosynthetic growth of strains expressing both LH1c and LH2 did not provide proof that RC–LH1 complexes assembled from LH1c could support photosynthetic growth, and so growth of the equivalent strains lacking LH2 was also studied. In all three LH2-deficient strains it could be concluded that the chimeric complexes were functional, as evidenced by a phase of strong photosynthetic growth that followed a lag of ~60–80 h (Fig. 4B). In addition, for strains RCLH1cXc-g and RCLH1cXd-g there was an initial phase of relatively weak photosynthetic growth (Fig, 4B) that was attributed to the population of free RCs on the basis that strikingly similar growth was obtained with an antenna-deficient strain (Fig. 4C). This result mirrored findings reported previously for an equivalent set of strains expressing native red/brown carotenoids [41].

An interesting question thrown up by these data is why initial photosynthetic growth supported by a population of free RCs was seen in strains with PufXc or no PufX, but was not seen in the strain with PufXs, despite clear evidence for the presence of comparable populations of free RCs in the latter strain. None of the data gathered to date throws light on this, but possibly there is a molecular interaction between PufXs and free *Rba. sphaeroides* RCs that somehow interferes with the ability of the latter to support photosynthetic growth, but this inhibitory interaction does not occur when PufXc is present, or either PufX is absent.

4.8. PufX-deficient chimeric RC–LH1 complexes can support photosynthetic growth

When LH1c was expressed in *Rba. sphaeroides* in the absence of either PufX the monomeric RC–LH1 complexes that were assembled had the elevated A_{LH1}/A_{RC} that is also characteristic of PufX-deficient *Rba. sphaeroides* RC–LH1 complexes. As in the latter it is known that the ring of LH1 BChls surrounding the RC is enlarged and complete, it seems reasonable to conclude that the structure of the chimeric PufX-deficient RC–LH1 complexes was similar, with a closed ring of LH1c pigment protein surrounding a central *Rba. sphaeroides* RC. However, despite this the PufX-deficient chimeric RC–LH1 complexes were capable of supporting photosynthetic growth (Fig. 4B) whereas the PufX-deficient *Rba. sphaeroides* RC–LH1 complexes were not (Fig. 4A). Thus it would appear that although the two types of PufX-deficient RC–LH1 complex may have been similar in composition, with an enlarged and (presumably) closed antenna, there is a crucial functional difference in that the chimeric complex can support photosynthetic growth whereas the purely *Rba. sphaeroides* complex cannot (unless the structure of its antenna is altered through a suppression mutation).

Although it was initially thought that the presence of a "closed" ring of LH1 around the RC in PufX-deficient strains of *Rba. sphaeroides* might provide a physical blockage to the diffusion of quinone in and out of the RC–LH1 complex, Comayras and co-workers [34] have shown that impairment of quinone diffusion is modest, and have concluded rather that the most serious consequence of a lack of PufXs is disruption of the correct operation of the Q_B site by a component of LH1s, such that there is a stabilization of Q_B^- and a shift in the equilibrium of the reaction $Q_A^- Q_B^- + 2H^+ \rightarrow Q_A Q_B H_2$ in favour of the reactant state. The result of this is that Q_A is more easily reduced when the intramembrane ubiquinone pool is reduced (such as would be the case under anaerobic/illuminated growth conditions), leading to the closure of RCs and a loss of photosynthetic capacity. The cause of this stabilization of Q_B^- is unclear, but it is assumed that it is due to a molecular interaction between the RC and a protein or cofactor component of LH1 that is normally prevented by PufX. The fact that photosynthetic growth is still supported by PufX-deficient chimeric RC–LH1 complexes suggests that this stabilization is not replicated by LH1c when either PufX is absent.

4.9. How does PufX manage the composition of the LH1 aggregate?

One finding underscored by the experiments described above is that in all the PufX-containing bacteria studied, including those *Rba. sphaeroides* strains expressing LH1c, aggregation of LH1 pigment proteins around the RC was restricted, producing an A_{LH1}/A_{RC} of 3.7 to 4.9, whereas in the PufX-deficient strains a more extensive aggregation of LH1 around the RC was obtained, producing a higher A_{LH1}/A_{RC} of 5.6 to 6.3. This suggests that PufX has some mechanism for interacting with both ends of the C-shaped LH1 antenna observed in *Rhodobacter* RC–LH1 monomers. In fact the effect of PufXs and PufXc on aggregation of LH1 α- and β-polypeptides and BChl *in vitro* has been studied by Loach and co-workers [67,68]. PufXc was found to inhibit formation of LH1-like aggregates formed from *Rba. capsulatus* LH1 α- and β-polypeptides (the BChls of which absorb around 872 nm). Likewise, PufXs was found to inhibit formation of LH1-like aggregates formed from *Rba. sphaeroides* LH1 α- and β-polypeptides, and there was also a small amount of cross-inhibition (15%) [67]. PufX was found to co-migrate with the corresponding LH1 α-polypeptide during purification in this study, indicating affinity between the two, but did not inhibit formation of homodimers that can be formed by the *Rba. sphaeroides* LH1 β-polypeptide in the presence of BChl [67]. In a subsequent study formation of LH1-like aggregates was inhibited to a significant extent by peptides corresponding to the membrane-embedded portion of PufX, again interacting with the α-polypeptide [68].

The picture that emerges is one in which the transmembrane helical region of PufX has a propensity to interact with the α-polypeptides that form the inner protein cylinder of the LH1 antenna, providing a mechanism to limit the extent of aggregation of the LH1 pigment protein around the RC. Conclusions based on these inhibition assays correspond well to the location of a possible PufX homolog in the 4.8 Å-resolution X-ray crystal structure of the monomeric RC–LH1 complex from *Rhodopseudomonas* (*Rps.*) *palustris* (PDB entry 1PYH), which is the highest resolution structure for a RC–LH1 complex currently available [3]. Fig. 8B shows a view of the 1PYH structure in the plane of the membrane, with the RC shown as a solid object with the H-polypeptide highlighted in dark grey. The RC is surrounded by an LH1 antenna comprising an inner ring of 15 α-polypeptides (cyan ribbons in Fig. 8B), an intervening ring of 30 BChls (spheres — alternating red/orange for adjacent BChls) and an outer ring of 15 β-polypeptides (magenta ribbons) that all follow the elliptical cross-section of the central RC. This LH1 pigment-protein ring is incomplete, with a gap in the middle of the long axis of the RC on the opposite side to the membrane-spanning α-helix of the RC H-polypeptide. An additional transmembrane α-helix of uncertain origin, termed helix W (yellow ribbon), is modelled into

density in this gap between LH1 α-polypeptides, and it is speculated that this protein may be a functional analogue of PufX [3]. This structure is in accord with low-resolution structural information from AFM of intact *Rps. palustris* membranes which also shows the RC surrounded by an incomplete ring of LH1 pigment protein [69].

4.10. A possible model for Rhodobacter RC–LH1 monomers and dimers

Given the observations in this report, in Fig. 8 we propose a specific structural arrangement through which PufX could manage the aggregation of the LH1 antenna around the RC in all *Rhodobacter* species and, in a subset of those species, promote the assembly of dimers in a manner which does not require structural rearrangement of each monomer. The *in silico* model shown in Fig. 8A is of a monomer of the *Rba. sphaeroides* RC–LH1 complex, and is based on the 4.8 Å-resolution X-ray crystal structure for the *Rps. palustris* RC–LH1 complex shown in Fig. 8B (PDB ID 1PYH). Given the limited resolution of the source data, all polypeptide chains included in structure 1PYH were modelled as poly-alanine, only the membrane-spanning helices of the LH1 polypeptides were included, again as poly-alanine, and the quinone cofactors of the RC were not included [3]. For the purposes of constructing the model depicted in Fig. 8A the 1PYH structure was first modified by replacing the RC component with the structure of a *Rba. sphaeroides* RC containing both quinones, achieved by aligning the two RC structures in PyMOL [70]. The surface-exposed isoprenoid side-chain of the Q_B quinone is shown as dark-teal sticks in Fig. 8B, to the left of the yellow helix of the W-polypeptide, and the approximate location of the buried headgroup is marked.

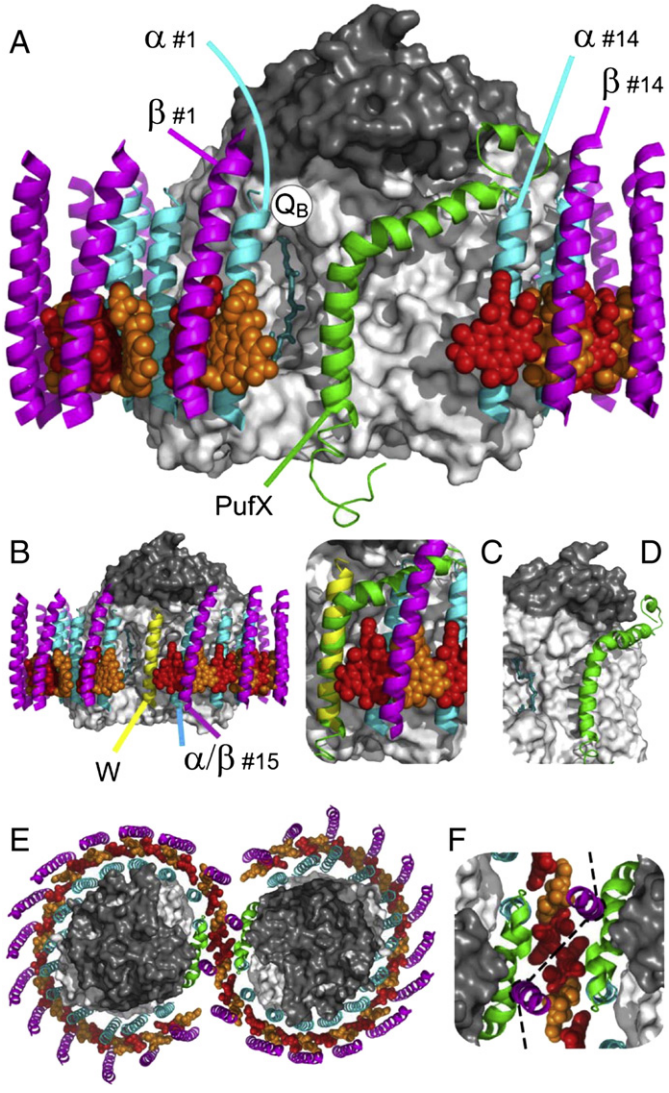

Fig. 8. Proposed model of monomeric and dimeric RC–LH1 complexes from *Rba. sphaeroides*. (A) Model of RC–LH1 monomer-containing PufXs and 14 pairs of LH1 α- and β-polypeptides, viewed in the plane of the membrane. (B) Equivalent view of the X-ray crystal structure of the *Rps. palustris* RC–LH1 complex, containing a W-polypeptide and 14 pairs of LH1 α- and β-polypeptides. (C) Close-up view of an overlay of PufXs with the W-polypeptide, showing a steric clash with LH1 α-polypeptide #15. (D) View of PufXs binding to the intramembrane surface of the RC. (E) View from the cytoplasmic side of the membrane of a model of a dimer of the *Rba. sphaeroides* RC–LH1 complex. (F) Close-up view of the dimer interface (dotted line). In all panels the RC is shown as a solid object with the largely extra-membrane H-polypeptide highlighted in dark grey. BChls are shown as spheres coloured alternating red and orange, LH1 α- and β-polypeptides as cyan or magenta ribbons, respectively, PufXs as a green ribbon and the *Rps. palustris* W-polypeptide as a yellow ribbon. The Q_B ubiquinone is shown as teal sticks in (A) and (B).

The membrane-spanning helix of the *Rps. palustris* W-polypeptide (Fig. 8B, yellow ribbon) was used as a guide for positioning of PufXs in the model of the *Rba. sphaeroides* RC–LH1 complex (Fig. 8A). Two NMR structures are available for purified PufXs in organic solvent, determined by Tunnicliffe and co-workers (PDB ID: 2NRG [71]) and Wang and co-workers (PDB ID: 2DW3 [72]). In both structures the central region of PufXs between Asn X13 and Met X53 forms an α-helix that could span a bilayer membrane, although at 41 amino acids this helix is much longer than the 20–25 amino acids that is more typical for a membrane-spanning α-helix in a single-pass membrane protein. In the NMR structure of Wang and co-workers this region forms a single, straight helix, but in the structure of Tunnicliffe and co-workers the helix exhibits a ~120° bend roughly in the middle that would allow the entire helical region to be accommodated within the ~40 Å span of a membrane, the C-terminal half running perpendicular to the membrane-plane and the N-terminal half running laterally in the lipid headgroup region on the cytoplasmic side of the membrane, at an angle of ~30° to the plane of the membrane. Evidence in support of this latter arrangement has recently been supplied by the observation that PufX has the same bent helical structure in a detergent micelle, and the finding that mutation of a Gly residue at a critical appressed position on the inside of the bend to progressively larger side-chains causes increasing loss of PufX from the membrane and a shift to a PufX-deficient phenotype [31]. This Gly at position 29 is one of only eight residues that are absolutely conserved in the five reported sequences for PufX [31], providing circumstantial evidence that this bent helical structure is a common feature of PufX proteins from different species. Given these considerations, PufX was introduced into the model of the *Rba. sphaeroides* RC–LH1 monomer using the 2NRG structure of Tunnicliffe and co-workers [31].

The helical region of the 2NRG structure of PufXs was added in the simplest possible way, by overlaying the C-terminal half of its bent α-helix with the periplasmic half of the membrane-spanning helix of the W-polypeptide (i.e. the bottom half of the yellow ribbon in the view shown in Fig. 8B). An enlarged view of this overlay is shown in Fig. 8C. The C-terminal half of the helix of PufXs was then rotated around its helical axis until the N-terminal half approached the intramembrane surface of the RC, as shown in Fig. 8C. This arrangement took into account the known N-in/C-out topology of PufX [73] and the fact that the protein shows affinity for binding to the RC as well as LH1, with strongest affinity seen when the RC and LH1 are both present [73]. Placement of PufXs in the position shown in Fig. 8C caused a strong steric clash between the N-terminal region of its helix and LH1 α-polypeptide #15 (labelled in Fig. 8B), shown in centre view as a cyan ribbon in Fig. 8C, and so to give the final model of a *Rba. sphaeroides* PufX-containing monomer shown in Fig. 8A, α-polypeptide #15 and the partner β-polypeptide (magenta ribbon) were removed, along with their associated BChl cofactors. In this final model the LH1 antenna comprised 14 pairs of α- and β-polypeptides, liganding a ring of 28 BChls. It differs from the *Rps. palustris* structure shown in Fig. 8B only in that PufXs has replaced helix W, and LH1 helices α15 and β15 and associated BChls have been removed.

A feature of note in the model shown in Fig. 8A is that the bend in the PufX helix serves two functions; it allows PufX to interact with two widely-spaced α-helices of the ring of LH1 α-polypeptides (numbered 1 and 14 in Fig. 8A), and it also allows the lateral, N-terminal half of the helix of PufXs to tuck-in underneath a very pronounced overhang formed by the extra-membrane domain of the H-polypeptide of the RC (highlighted in dark grey at the top of Fig. 8A). An alternative view of this arrangement to emphasize the latter point is shown in Fig. 8D; relative to Fig. 8A the structure is rotated around the vertical axis from left to right and the LH1 components removed. The helix of PufX sits against the intramembrane surface of the RC formed by the L- and M-polypeptides (Fig. 8D), and the N-terminal portion fits neatly under the H-polypeptide domain. It should also be noted that the helix of PufX is on the same side of the RC as the entrance to the Q_B site, the isoprenoid side-chain of the Q_B quinone emerging from the Q_B pocket being visible as dark-teal sticks in Fig. 8A, just to the left of the membrane-spanning portion of PufXs. This positioning is consistent with a number of observations that implicate PufX in ensuring normal operation of the Q_B site during quinone reduction and cyclic electron transfer [34–36].

The model shown in Fig. 8A leads to a mechanism for PufX to determine the aggregation state of the LH1 antenna. An interaction between the membrane-spanning helix of PufX and LH1α polypeptide #1 would provide a means to "cap" that end of the C-shaped antenna and an interaction between the N-terminal region of the lateral helix of PufX and LH1α polypeptide #14 would provide a means to cap the other end. It seems plausible that the non-helical regions at the N- and C-termini of PufX, which are unstructured in the available NMR structures of the purified PufXs, could further interact with the LH1 α/β pairs at positions #14 and #1, respectively. Furthermore, prevention of aggregation of LH1 beyond α/β pair #14 creates a structure for the monomer that, in some species, could then lead to the formation of a dimer of the form that has been visualized through EM and AFM, with two RCs linked by an S-shaped antenna. A model of an RC–LH1 dimer, constructed using data from single particle cryo-EM of the dimeric *Rba. sphaeroides* RC–LH1 complex as a guide [57] is shown in Fig. 8E. Cryo-EM has shown that when the dimer is viewed in the plane of the membrane, and perpendicular to its long axis, the two monomers are tilted away from one another at a mutual angle of 34° [57]. Accordingly, to construct a model of a dimeric RC–LH1 complex the monomer shown in Fig. 8A was rotated by 90° around the horizontal axis from top to bottom to provide a view of its cytoplasmic face. It was then rotated anticlockwise around the axis perpendicular to the page until α/β polypeptide pair #14 was positioned just above the horizontal, as shown in the left half of Fig. 8E. The monomer was then tilted around the vertical axis from right to left by 17°, duplicated, the second copy rotated 180° around the axis perpendicular to the page, and the two monomers brought together to form a symmetrical dimer (Fig. 8E), the interface being formed by LH1 α/β pair #14 and the N-terminus of PufX. The two monomers were positioned in such a way that the spacing between the two α-polypeptides and two β-polypeptides at the interface, shown in close-up view in Fig. 8F, was similar to that between adjacent polypeptides in the remainder of the antenna, the two BChls at the interface did not overlap, and overall the antenna formed an unbroken inverted S-shape. The dotted line in Fig. 8F denotes the interface between symmetrically-arranged monomers, the green ribbon showing how the N-terminal region of PufX is suitably positioned to engage in molecular interactions with LH1 polypeptides in this interface region. Clearly, truncation of the N-terminus of PufX would change the structure of this interface, and conceivably interfere with the formation of dimers, as is observed experimentally [57].

A similar "managing" of the aggregation state of LH1 by a PufXs with the structure reported by Wang and co-workers [72], with a central, straight 41 amino acid α-helix, would not be possible if it is assumed that it crosses the membrane in the approximately perpendicular manner indicated by the *Rps. palustris* W-polypeptide. Such an arrangement would not provide any obvious means for PufX to interact with LH1 α-polypeptides spaced apart in the manner shown in Fig. 8A, and such a helix would engage in steric clashes with the H-polypeptide and be almost twice as long as that typically observed for a membrane-spanning helix.

4.11. Comparisons with published models for Rhodobacter RC–LH1 dimers

Two principal models have been proposed for a dimeric RC–LH1 complex, that differ in the assigned location of PufX. The first, based on cryo-EM of 2D crystals of the dimeric *Rba. sphaeroides* complex [57] and AFM of membranes [18] from *Rba. blasticus* places two symmetrically-arranged molecules of PufX at the very centre of the dimer, providing a buffer between the two halves of the LH1 antenna. This assignment has been used *in silico* models of the RC–LH1 dimer [62], using the "straight helix" NMR structure for PufXs, and inspired proposals that PufXs dimerisation initiates assembly of the entire RC–LH1 complex [18]. The second, based on EM of 2D crystals of *Rba. sphaeroides* dimers [15], places the C-terminal half of the α-helix of a bent PufX roughly in the position occupied by LH1 α-polypeptide #1 in the model shown in Fig. 8A, adjacent to the Q_B site of the RC and between the RC and the terminal α/β pair of LH1 which sit further out from the surface of the RC. The N-terminal half of PufX is proposed to angle across towards the dimer interface to make interactions with β- and α-polypeptides of the other half of the dimer [31].

The location of PufX in the model shown in Fig. 8A is different from both of these, being guided by the position of the W-polypeptide in the *Rps. palustris* RC–LH1 complex. The assigned position of the membrane-spanning half of the PufX helix in the model in Fig. 8A is similar to that occupied by region of density pointed out by Qian and co-workers in electron diffraction studies of 2D crystals of *Rba. sphaeroides* dimers, and tentatively assigned to the N-terminal half of PufX [15]. Thus the main difference between the model shown in Fig. 8A and that of Qian and co-workers is that in the present model the membrane-spanning portion of PufX is further from the Q_B site and closer to the dimer interface, which would allow the N-terminus of PufX to interact with the LH1 proteins from its own half of the dimer, rather than reaching across to interact with LH1 proteins from the second monomer. This would allow PufX to facilitate dimerisation in a fashion that does not require structural rearrangement of the monomer, the dimerisation surface of each monomer being formed by a combination of LH1 α- and β-polypeptides and the N-terminus of PufX.

5. Conclusions

The findings presented in this study help to tease apart the different functions of PufX in different species of *Rhodobacter*.

First, we propose that in all species of *Rhodobacter* PufX defines the composition of the monomeric RC–LH1 complex, managing the aggregation state of the LH1 pigment protein around the RC and determining the position of the break in the continuity of the LH1 cylinder relative to the entrance of the Q_B pocket of the RC. We would contend that in *Rhodobacter* the bent structure of the long membrane-embedded PufX helix is a conserved feature of its structure that serves to limit the aggregation state of LH1 to 14 pairs of α/β-polypeptides and 28 BChls, maintaining a wider gap in the LH1 ring than is seen in *Rps. palustris*. This management of LH1 is achieved by the C-terminal portion of the α-helix of PufX binding to the RC at a particular position approximately symmetrical to the membrane-spanning α-helix of the H-polypeptide, fixing the position of one end of the LH1 antenna, and the N-terminal portion of the PufX α-helix angling across the intramembrane surface of the RC to interact with the other end of the LH1 antenna.

Second, in *Rba. sphaeroides*, probably also in *Rba. capsulatus*, and possibly in other *Rhodobacter* species, in carrying out its function of

limiting aggregation of LH1 around the RC, PufX prevents a molecular interaction between the two that would disturb the correct operation of the two-electron gate facilitated by the RC quinones. It is known that PufX-deficient strains of *Rba. sphaeroides* and *capsulatus* are non-photosynthetic, and there is a specific proposal that this is due to disturbances in the native properties of the Q_B and Q_A sites in *Rba. sphaeroides*. One insight provided by the present study is that this molecular interaction may be species-specific, as PufX-deficient RC–LH1 complexes containing (presumably a closed ring of) LH1c appeared to be capable of supporting photosynthetic growth. The nature of this interaction is not clear, but in addition to a direct LH1–RC protein–protein it could include an involvement of carotenoid and/or lipid.

Third, in a subset of species, including *Rba. sphaeroides*, *azotoformans*, *blasticus* and *changlensis*, a dimeric form of the RC–LH1 complex is assembled, with PufX facilitating the formation of this dimeric form in *Rba. sphaeroides* and possibly in the other species. Interaction of the N-terminal region of PufX with the LH1 α- and β-polypeptides from its own monomer at the dimer interface would provide a means for PufX to influence the formation of contacts between monomers without having to significantly change their structure. The physiological advantages of the dimeric form of the RC–LH1 complex are not clear, but it is clear that species or strains appearing to assemble exclusively monomeric RC–LH1 complexes are not impaired in photosynthetic growth.

Finally, evidence has been presented that the dimeric form of the RC–LH1 complex does not assemble in *Rba. veldkampii*, and on the basis of the data above from native and chimeric strains we would contend that the same is likely to be true for the complexes from *Rba. capsulatus* and *Rba. vinaykumarii*. This contention requires validation through a technique such as AFM that can image monomeric and dimeric RC–LH1 complexes in intact membranes.

Supplementary materials related to this article can be found online at doi:10.1016/j.bbabio.2011.10.009.

Acknowledgements

The authors acknowledge the Biotechnology and Biological Sciences Research Council of the United Kingdom for funding.

References

[1] X. Hu, A. Damjanovic, T. Ritz, K. Schulten, Architecture and mechanism of the light-harvesting apparatus of purple bacteria, Proc. Natl. Acad. Sci. U. S. A. 95 (1998) 5935–5941.
[2] X. Hu, T. Ritz, A. Damjanovic, F. Autenrieth, K. Schulten, Photosynthetic apparatus of purple bacteria, Q. Rev. Biophys. 35 (2002) 1–62.
[3] A.W. Roszak, T.D. Howard, J. Southall, A.T. Gardiner, C.J. Law, N.W. Isaacs, R.J. Cogdell, Crystal structure of the RC–LH1 core complex from *Rhodopseudomonas palustris*, Science 302 (2003) 1969–1972.
[4] R.J. Cogdell, A.T. Gardiner, A.W. Roszak, C.J. Law, J. Southall, N.W. Isaacs, Rings, ellipses and horseshoes: how purple bacteria harvest solar energy, Photosynth. Res. 81 (2004) 207–214.
[5] C.J. Law, A.W. Roszak, J. Southall, A.T. Gardiner, N.W. Isaacs, R.J. Cogdell, The structure and function of bacterial light-harvesting complexes (Review), Mol. Membr. Biol. 21 (2004) 183–191.
[6] S. Scheuring, D. Levy, J.L. Rigaud, Watching the components of photosynthetic bacterial membranes and their *in situ* organisation by atomic force microscopy, Biochim. Biophys. Acta 1712 (2005) 109–127.
[7] R.J. Cogdell, A. Gall, J. Kohler, The architecture and function of the light-harvesting apparatus of purple bacteria: from single molecules to *in vivo* membranes, Q. Rev. Biophys. 39 (2006) 227–324.
[8] S. Scheuring, AFM studies of the supramolecular assembly of bacterial photosynthetic core-complexes, Curr. Opin. Chem. Biol. 10 (2006) 387–393.
[9] J.N. Sturgis, J.D. Tucker, J.D. Olsen, C.N. Hunter, R.A. Niederman, Atomic force microscopy studies of native photosynthetic membranes, Biochemistry 48 (2009) 3679–3698.
[10] M.R. Jones, Bacterial photosynthesis, Photobiological Sciences Online, American Society for Photobiology, 2009.
[11] G. McDermott, S.M. Prince, A.A. Freer, A.M. Hawthornthwaite-Lawless, M.Z. Papiz, R.J. Cogdell, N.W. Isaacs, Crystal structure of an integral membrane light-harvesting complex from photosynthetic bacteria, Nature 374 (1995) 517–521.
[12] J. Koepke, X. Hu, C. Muenke, K. Schulten, H. Michel, The crystal structure of the light-harvesting complex II (B800-850) from *Rhodospirillum molischianum*, Structure 4 (1996) 581–597.
[13] C. Jungas, J.L. Ranck, J.L. Rigaud, P. Joliot, A. Vermeglio, Supramolecular organization of the photosynthetic apparatus of *Rhodobacter sphaeroides*, EMBO J. 18 (1999) 534–542.
[14] C.A. Siebert, P. Qian, D. Fotiadis, A. Engel, C.N. Hunter, P.A. Bullough, Molecular architecture of photosynthetic membranes in *Rhodobacter sphaeroides*: the role of PufX, EMBO J. 23 (2004) 690–700.
[15] P. Qian, C.N. Hunter, P.A. Bullough, The 8.5 angstrom projection structure of the core RC–LH1–PufX dimer of *Rhodobacter sphaeroides*. J. Biol. Chem. 349 (2005) 948–960.
[16] S. Bahatyrova, R.N. Frese, C.A. Siebert, J.D. Olsen, K.O. Van Der Werf, R. Van Grondelle, R.A. Niederman, P.A. Bullough, C. Otto, C.N. Hunter, The native architecture of a photosynthetic membrane, Nature 430 (2004) 1058–1062.
[17] S. Scheuring, F. Francia, J. Busselez, B.A. Melandri, J.L. Rigaud, D. Levy, Structural role of PufX in the dimerization of the photosynthetic core complex of *Rhodobacter sphaeroides*, J. Biol. Chem. 279 (2004) 3620–3626.
[18] S. Scheuring, J. Busselez, D. Levy, Structure of the dimeric PufX-containing core complex of *Rhodobacter blasticus* by *in situ* atomic force microscopy, J. Biol. Chem. 280 (2005) 1426–1431.
[19] L.N. Liu, J.N. Sturgis, S. Scheuring, Native architecture of the photosynthetic membrane from *Rhodobacter veldkampii*, J. Struct. Biol. 173 (2011) 138–145.
[20] J. Busselez, M. Cottevieille, P. Cuniasse, F. Gubellini, N. Boisset, D. Levy, Structural basis for the PufX-mediated dimerization of bacterial photosynthetic core complexes, Structure 15 (2007) 1674–1683.
[21] K. Holden-Dye, L.I. Crouch, M.R. Jones, Structure, function and interactions of the PufX protein, Biochim. Biophys. Acta 1777 (2008) 613–630.
[22] T. Walz, S.J. Jamieson, C.M. Bowers, P.A. Bullough, C.N. Hunter, Projection structures of three photosynthetic complexes from *Rhodobacter sphaeroides*: LH2 at 6 Å, LH1 and RC–LH1 at 25 Å, J. Mol. Biol. 282 (1998) 833–845.
[23] S.J. Jamieson, P. Wang, P. Qian, J.Y. Kirkland, M.J. Conroy, C.N. Hunter, P.A. Bullough, Projection structure of the photosynthetic reaction centre–antenna complex of *Rhodospirillum rubrum* at 8.5 Å resolution. EMBO J. 21 (2002) 3927–3935.
[24] S. Scheuring, J. Seguin, S. Marco, D. Levy, B. Robert, J.L. Rigaud, Nanodissection and high-resolution imaging of the *Rhodopseudomonas viridis* photosynthetic core complex in native membranes by AFM, Proc. Natl. Acad. Sci. U. S. A. 100 (2003) 1690–1693.
[25] D. Fotiadis, P. Qian, A. Philippsen, P.A. Bullough, A. Engel, C.N. Hunter, Structural analysis of the reaction center light-harvesting complex I photosynthetic core complex of *Rhodospirillum rubrum* using atomic force microscopy, J. Biol. Chem. 279 (2004) 2063–2068.
[26] S. Scheuring, J.N. Sturgis, Chromatic adaptation of photosynthetic membranes, Science 309 (2005) 484–487.
[27] R.P. Goncalves, A. Bernadac, J.N. Sturgis, S. Scheuring, Architecture of the native photosynthetic apparatus of *Phaeospirillum molischianum*, J. Struct. Biol. 152 (2005) 221–228.
[28] G. Klug, S.N. Cohen, Pleiotropic effects of localized *Rhodobacter capsulatus puf* operon deletions on production of light-absorbing pigment-protein complexes, J. Bacteriol. 170 (1988) 5814–5821.
[29] J.W. Farchaus, H. Gruenberg, D. Oesterhelt, Complementation of a reaction center-ceficient *Rhodobacter sphaeroides pufLMX* deletion strain in trans with *pufBALM* does not restore the photosynthesis-positive phenotype, J. Bacteriol. 172 (1990) 977–985.
[30] T.G. Lilburn, C.E. Haith, R.C. Prince, J.T. Beatty, Pleiotropic effects of PufX gene deletion on the structure and function of the photosynthetic apparatus of *Rhodobacter capsulatus*, Biochim. Biophys. Acta 1100 (1992) 160–170.
[31] E.C. Ratcliffe, R.B. Tunnicliffe, I.W. Ng, P.G. Adams, P. Qian, K. Holden-Dye, M.R. Jones, M.P. Williamson, C.N. Hunter, Experimental evidence that the membrane-spanning helix of PufX adopts a bent conformation that facilitates dimerisation of the *Rhodobacter sphaeroides* RC–LH1 complex through N-terminal interactions, Biochim. Biophys. Acta 1807 (2011) 95–107.
[32] F. Francia, J. Wang, H. Zischka, G. Venturoli, D. Oesterhelt, Role of the N- and C-terminal regions of the PufX protein in the structural organization of the photosynthetic core complex of *Rhodobacter sphaeroides*, Eur. J. Biochem. 269 (2002) 1877–1885.
[33] P.G. Adams, D.J. Mothersole, I.W. Ng, J.D. Olsen, C.N. Hunter, Monomeric RC–LH1 core complexes retard LH2 assembly and intracytoplasmic membrane formation in PufX-minus mutants of *Rhodobacter sphaeroides*, Biochim. Biophys. Acta 1807 (2011) 1044–1055.
[34] F. Comayras, C. Jungas, J. Lavergne, Functional consequences of the organization of the photosynthetic apparatus in *Rhodobacter sphaeroides*: II. A study of PufX-membranes, J. Biol. Chem. 280 (2005) 11214–11223.
[35] W.P. Barz, F. Francia, G. Venturoli, B.A. Melandri, A. Vermeglio, D. Oesterhelt, Role of PufX protein in photosynthetic growth of *Rhodobacter sphaeroides*.1. PufX Is required for efficient light-driven electron-transfer and photophosphorylation under anaerobic conditions, Biochemistry 34 (1995) 15235–15247.
[36] W.P. Barz, A. Vermeglio, F. Francia, G. Venturoli, B.A. Melandri, D. Oesterhelt, Role of the PufX protein in photosynthetic growth of *Rhodobacter sphaeroides*. 2. PufX is required for efficient ubiquinone ubiquinol exchange between the reaction-center QB site and the cytochrome bc1 complex, Biochemistry 34 (1995) 15248–15258.
[37] F. Francia, J. Wang, G. Venturoli, B.A. Melandri, W.P. Barz, D. Oesterhelt, The reaction center–LH1 antenna complex of *Rhodobacter sphaeroides* contains one PufX molecule which is involved in dimerization of this complex, Biochemistry 38 (1999) 6834–6845.
[38] Y. Tsukatani, K. Matsuura, S. Masuda, K. Shimada, A. Hiraishi, K.V.P. Nagashima, Phylogenetic distribution of unusual triheme to tetraheme cytochrome subunit in the reaction center complex of purple photosynthetic bacteria, Photosynth. Res. 79 (2004) 83–91.

[39] P. Anil Kumar, T.N. Srinivas, C. Sasikala, V.Ch. Ramana, *Rhodobacter changlensis* sp. nov., a psychrotolerant, phototrophic alphaproteobacterium from the Himalayas of India, Int. J. Syst. Evol. Microb. 57 (2007) 2568–2571.
[40] T.N. Srinivas, P.A. Kumar, C. Sasikala, V.Ch. Ramana, J.F. Imhoff, *Rhodobacter vinaykumarii* sp. nov., a marine phototrophic alphaproteobacterium from tidal waters, and emended description of the genus *Rhodobacter*, Int. J. Syst. Evol. Microb. 57 (2007) 1984–1987.
[41] T.K. Fulcher, J.T. Beatty, M.R. Jones, Demonstration of the key role played by the PufX protein in the functional and structural organization of native and hybrid bacterial photosynthetic core complexes, J. Bacteriol. 180 (1998) 642–646.
[42] M.R. Jones, G.J. Fowler, L.C. Gibson, G.G. Grief, J.D. Olsen, W. Crielaard, C.N. Hunter, Mutants of *Rhodobacter* sphaeroides lacking one or more pigment-protein complexes and complementation with reaction-centre, LH1, and LH2 genes, Mol. Microbiol. 6 (1992) 1173–1184.
[43] C.N. Hunter, G. Turner, Transfer of genes coding for apoproteins of reaction center and light-harvesting LH1 complexes to *Rhodobacter sphaeroides*, J. Gen. Microbiol. 134 (1988) 1471–1480.
[44] J.T. Beatty, H. Gest, Generation of succinyl-coenzyme-a in photosynthetic bacteria, Arch. Microbiol. 129 (1981) 335–340.
[45] C.N. Hunter, P. Mcglynn, M.K. Ashby, J.G. Burgess, J.D. Olsen, DNA sequencing and complementation deletion analysis of the *bcha-puf* operon region of *Rhodobacter sphaeroides*— *in vivo* mapping of the oxygen-regulated *puf* promoter, Mol. Microbiol. 5 (1991) 2649–2661.
[46] L.I. Crouch, K. Holden-Dye, M.R. Jones, Dimerisation of the *Rhodobacter sphaeroides* RC–LH1 photosynthetic complex is not facilitated by a GxxxG motif in the PufX polypeptide, Biochim. Biophys. Acta 1797 (2010) 1812–1819.
[47] M.R. Jones, M. Heer-Dawson, T.A. Mattioli, C.N. Hunter, B. Robert, Site-specific mutagenesis of the reaction centre from *Rhodobacter sphaeroides* studied by Fourier transform Raman spectroscopy: mutations at tyrosine M210 do not affect the electronic structure of the primary donor, FEBS Lett. 339 (1994) 18–24.
[48] F. Gubellini, F. Francia, J. Busselez, G. Venturoli, D. Levy, Functional and structural analysis of the photosynthetic apparatus of *Rhodobacter veldkampii*, Biochemistry 45 (2006) 10512–10520.
[49] M.R. Jones, R.W. Visschers, R. van Grondelle, C.N. Hunter, Construction and characterization of a mutant of *Rhodobacter sphaeroides* with the reaction center as the sole pigment-protein complex, Biochemistry 31 (1992) 4458–4465.
[50] P. McGlynn, C.N. Hunter, M.R. Jones, The *Rhodobacter sphaeroides* PufX protein is not required for photosynthetic competence in the absence of a light harvesting system, FEBS Lett. 349 (1994) 349–353.
[51] C.N. Hunter, J.D. Pennoyer, J.N. Sturgis, D. Farrelly, R.A. Niederman, Oligomerization states and associations of light-harvesting pigment protein complexes of *Rhodobacter sphaeroides* as analyzed by lithium dodecyl-sulfate polyacrylamide-gel electrophoresis, Biochemistry 27 (1988) 3459–3467.
[52] A. Oz, G. Sabehi, M. Koblizek, R. Massana, O. Beja, Roseobacter-like bacteria in Red and Mediterranean Sea aerobic anoxygenic photosynthetic populations, Appl. Environ. Microbiol. 71 (2005) 344–353.
[53] L.A. Waidner, D.L. Kirchman, Aerobic anoxygenic photosynthesis genes and operons in uncultured bacteria in the Delaware River, Environ. Microbiol. 7 (2005) 1896–1908.
[54] T.E. Meyer, J.A. Kyndt, M.A. Cusanovich, Occurrence and sequence of Sphaeroides Heme Protein and diheme cytochrome C in purple photosynthetic bacteria in the family Rhodobacteraceae, BMC Biochem 11 (2010) 24.
[55] W.H. Westerhuis, J.N. Sturgis, E.C. Ratcliffe, C.N. Hunter, R.A. Niederman, Isolation, size estimates, and spectral heterogeneity of an oligomeric series of light-harvesting 1 complexes from *Rhodobacter sphaeroides*, Biochemistry 41 (2002) 8698–8707.
[56] P.J. Kiley, A. Varga, S. Kaplan, Physiological and structural analysis of light-harvesting mutants of *Rhodobacter sphaeroides*, J. Bacteriol. 170 (1988) 1103–1115.
[57] P. Qian, P.A. Bullough, C.N. Hunter, Three-dimensional reconstruction of a membrane-bending complex: the RC–LH1–PufX core dimer of *Rhodobacter sphaeroides*, J. Biol. Chem. 283 (2008) 14002–14011.
[58] G. Drews, Formation of the light-harvesting complex I (B870) of anoxygenic phototrophic purple bacteria, Arch. Microbiol. 166 (1996) 151–159.
[59] K.R. Girija, C. Sasikala, V. Ramana Ch, C. Sproer, S. Takaichi, V. Thiel, J.F. Imhoff, *Rhodobacter johrii* sp. nov., an endospore-producing cryptic species isolated from semi-arid tropical soils, Int. J. Syst. Evol. Microbiol. 60 (2010) 2099–2107.
[60] K. Eckersley, C.S. Dow, *Rhodopseudomonas blastica* Sp-Nov — a member of the Rhodospirillaceae, J. Gen. Microbiol. 119 (1980) 465–473.
[61] H. Kawasaki, Y. Hoshino, A. Hirata, K. Yamasato, Is intracytoplasmic membrane structure a generic criterion? It does not coincide with phylogenetic interrelationships among phototrophic purple nonsulfur bacteria, Arch. Microbiol. 160 (1993) 358–362.
[62] J. Hsin, C. Chipot, K. Schulten, A glycophorin A-Like framework for the dimerization of photosynthetic core complexes, JACS 131 (2009) 17096–+.
[63] M.A. Lemmon, J.M. Flanagan, H.R. Treutlein, J. Zhang, D.M. Engelman, Sequence specificity in the dimerization of transmembrane alpha-helices, Biochemistry 31 (1992) 12719–12725.
[64] M.A. Lemmon, H.R. Treutlein, P.D. Adams, A.T. Brunger, D.M. Engelman, A dimerization motif for transmembrane alpha-helices, Nat. Struct. Biol. 1 (1994) 157–163.
[65] D.K. Wong, W.J. Collins, A. Harmer, T.G. Lilburn, J.T. Beatty, Directed mutagenesis of the *Rhodobacter capsulatus puhA* gene and *orf 214*: pleiotropic effects on photosynthetic reaction center and light-harvesting 1 complexes, J. Bacteriol. 178 (1996) 2334–2342.
[66] P.R. Jaschke, H.N. Leblanc, A.S. Lang, J.T. Beatty, The PucC protein of *Rhodobacter capsulatus* mitigates an inhibitory effect of light-harvesting 2 alpha and beta proteins on light-harvesting complex 1, Photosynth. Res. 95 (2008) 279–284.
[67] P.A. Recchia, C.M. Davis, T.G. Lilburn, J.T. Beatty, P.S. Parkes-Loach, C.N. Hunter, P.A. Loach, Isolation of the PufX protein from *Rhodobacter capsulatus* and *Rhodobacter sphaeroides*: evidence for its interaction with the alpha-polypeptide of the core light-harvesting complex, Biochemistry 37 (1998) 11055–11063.
[68] P.S. Parkes-Loach, C.J. Law, P.A. Recchia, J. Kehoe, S. Nehrlich, J. Chen, P.A. Loach, Role of the core region of the PufX protein in inhibition of reconstitution of the core light-harvesting complexes of *Rhodobacter sphaeroides* and *Rhodobacter capsulatus*, Biochemistry 40 (2001) 5593–5601.
[69] S. Scheuring, R.P. Goncalves, V. Prima, J.N. Sturgis, The photosynthetic apparatus of *Rhodopseudomonas palustris*: structures and organization, J. Mol. Biol. 358 (2006) 83–96.
[70] W. DeLano, The PyMOL Molecular Graphics System, DeLano Scientific, San Carlos, CA, USA, 2002.
[71] R.B. Tunnicliffe, E.C. Ratcliffe, C.N. Hunter, M.P. Williamson, The solution structure of the PufX polypeptide from *Rhodobacter sphaeroides*, FEBS Lett. 580 (2006) 6967–6971.
[72] Z.Y. Wang, H. Suzuki, M. Kobayashi, T. Nozawa, Solution structure of the *Rhodobacter sphaeroides* PufX membrane protein: Implications for the quinone exchange and protein–protein interactions, Biochemistry 46 (2007) 3635–3642.
[73] R.J. Pugh, P. McGlynn, M.R. Jones, C.N. Hunter, The LH1–RC core complex of *Rhodobacter sphaeroides*: interaction between components, time-dependent assembly, and topology of the PufX protein, Biochim. Biophys. Acta 1366 (1998) 301–316.
[74] A. Bairoch, R. Apweiler, The SWISS-PROT protein sequence database and its supplement TrEMBL in 2000, Nucleic Acids Res. 28 (2000) 45–48.
[75] J.D. Thompson, T.J. Gibson, F. Plewniak, F. Jeanmougin, D.G. Higgins, The CLUSTAL_X windows interface: flexible strategies for multiple sequence alignment aided by quality analysis tools, Nucleic Acids Res. 25 (1997) 4876–4882.